KAULA, W.M.
Institute of Planetary & Space Sciences
University of California
Los Angeles California 90024
United States of America

Proc.Symposium on Earth's Gravitational Field & Secular Variations in Position (1973),240-247.

MANTLE CONVECTIVE MODELS RELATED TO THE GRAVITY FIELD AND TECTONIC MOTION

ABSTRACT

A comprehensive mantle convective flow model will not be forthcoming for a long time. Difficulties include the highly non-linear character of the problem, the strong temperature and stress dependence of mantle rheology, and the complexity of the lithospheric boundary condition. Considerable improvement is being made in understanding simplified models. The principal regions in which more geodetic data would be of value are

1. major fault zones,
2. interiors of seismically active continents, and
3. post-glacial rebound areas.

1. Introduction

It is a truism of science that the aim of science is to find the fundamental causes of phenomena. However, this truism is an insufficient guide to action; to say, for example, that the Earth's gravity field is one of many consequences of a "big bang" origin of the universe does not yield any insight. In practice, the causes we seek are those which are proximate enough that the processes connecting them to observable phenomena are reasonably comprehensible and incontrovertible.

For much geodetic data the dominant cause is well known: isostasy. However, at this late date, the prevalence of isostasy is not very interesting: mainly the manifestation of the fact that, over 4.6×10^9 years of Earth history, density irregularities which are isostatically compensated tend to persist, while those which are not tend to die away by rock creep.

Of more interest are the indicators of current activity within the Earth. Most significant are:

1. the 10^3 year time scale of post glacial adjustment;
2. the approximately 45 ergs/cm^2/sec of heat coming from below the crust;
3. the 10^7 year time scale of the current plate tectonic pattern indicated by sea floor remanent magnetism; and
4. the marked compositional differentiations associated with igneous activity.

The creep rate inferred from the post glacial data, together with the density of heat sources indicated by the heat flow, imply that the Earth's interior is a highly non-linear flow system. The much longer time scale of plate tectonics indicates that this flow system is close to steady state. The compositional differentiations suggests that compositional inhomogeneities may be as important in driving the flow as thermal effects. A further complication is that the distribution of radiogenic heat sources is strongly correlated with variations in the bulk chemical composition, the U, Th, K being normally associated with CaO and Al_2O_3 (DICKINSON & LUTH 1971; GAST 1972; WYLLIE 1973).

2. Fundamental Considerations

If we assume a constant linear viscous rheology (i.e., strain rate proportionate to stress); assume all the heat sources are associated with the minor component δn_A; assume incompressibility; let potential $V = V_o + \delta V$, density $\rho = \rho_o + \delta\rho$, pressure $p = p_o + \delta p$; and take $\delta\rho$ to be composed of a thermal part $-\rho_o \alpha\, \delta T$ and a compositional part $\Delta\rho\, \delta n_A$, then the momentum and energy equations become:

$$\rho\left(\dot{\underset{\sim}{v}} + \underset{\sim}{v}\cdot\nabla\underset{\sim}{v}\right) = \rho_o \nabla\delta V - \nabla\delta p + \underset{\sim}{\lambda}\, g\left(\rho_o\alpha\, \delta T - \Delta\rho\, \delta n_A\right) + \eta\, \nabla^2\underset{\sim}{v} \tag{1}$$

and

$$\dot{T} + \underset{\sim}{v}\cdot\nabla T = \kappa\, \nabla^2 T + \frac{q n_A}{\rho C_V} + \frac{\eta}{2\rho C_V} E^2 \tag{2},$$

where $\underset{\sim}{v}$ is velocity, $\underset{\sim}{\lambda}$ is the radial unit vector, g is gravity, η is viscosity, T is temperature, κ is thermal diffusivity, q is energy release per unit volume of heat sources n_A, C_V is heat capacity and E is the strain rate tensor.

If we further use as a unit of length the distance d between upper and lower boundaries; of time, d^2/κ; of mass, $d^2\eta/\kappa$; and of temperature, $q n_A d^2/(3\kappa\rho C_V)$, then the equations become

$$\frac{1}{Pr}\left(\dot{\underset{\sim}{v}} + \underset{\sim}{v}\cdot\nabla\underset{\sim}{v}\right) = \frac{1}{Pr}\delta V - \nabla\delta p + \underset{\sim}{\lambda}\left(Ra\, \delta T - Co\, \delta n_A\right) + \nabla^2\underset{\sim}{v} \tag{3},$$

and

$$\dot{T} + \underset{\sim}{v}\cdot\nabla T = \nabla^2 T + Di\, E^2 + 3\left(1 + \delta n_A/n_A\right) \tag{4},$$

where, using typical values for the Earth's mantle with $d \simeq 2900$ km,

$$\left.\begin{aligned} Pr &= \eta/(\rho_o\kappa) && \simeq 3\times 10^{24} \\ Ra &= \alpha q\, n_A d^5 g/(3\kappa^2\eta C_V) && \simeq 4\times 10^{7} \\ Co &= \Delta\rho\, g\, d^3/(\kappa\eta) && \simeq 10^{8} \\ Di &= 3\kappa^2\eta/(2q\, n_A d^4) = \alpha dg/(C_V Ra) && \simeq 10^{-8} \end{aligned}\right\} \tag{5},$$

The large Prandtl number Pr means that the flow is non-turbulent; evolution of the system from within takes place only through the energy equation. The large Rayleigh Ra, about 10^4 times critical, indicates the flow is highly non-linear, and the large Co indicates that compositional variations could be of comparable significance to thermal variations. The small Di suggests dissipation is negligible; however (unlike Pr), this parameter has a strong dependence on the length scale d. Furthermore, the strain rate tensor E depends strongly on the aspect ratio of the flow. Hence if the flow cells are confined to a relatively shallow zone of less than about 500 km, dissipation can be significant. This also corresponds roughly to the length d which will make the Rayleigh number Ra close to the value found as critical for the onset of convective flow, 1100.

Laboratory experiments indicate that the assumptions on which the aforegoing discussion is based may be a gross over-simplification (WEERTMAN 1970; STOCKER & ASHBY 1973). Assuming variations in

the gravity field Δg are due to density variations $\delta\rho$ spread over some zone h, the resulting stress differences of order $g\,\delta\rho\,h$ are large enough that the rock strain rate has a strongly non-linear dependence on stress, to a third or higher power of the stress. Furthermore, there are strongly non-linear dependences of viscosity η and density ρ on temperature, the latter arising from phase transitions. The most evident consequence of the temperature dependence of the viscosity is the lithosphere, a layer 30 - 100 km thick for which an elastic rheology is appropriate. The lithosphere is a strong stress guide horizontally, as evidenced by the wide extent of some of the tectonic plates. It also must have a strong thermal effect where it is thrust down into the asthenosphere. On the other hand, the lithosphere is rather thin on a global scale, so that it is not at all resistant to broad scale vertical stresses, and acts essentially as a free boundary.

Laboratory experiments and theoretical studies both indicate that contained heat sources and temperature dependence of properties have complicating effects, making stable patterns three-dimensional rather than two-dimensional (BUSSE 1967). As might be expected, the non-linear dependence of strain rate on stress has the effect of concentrating the flow considerably.

3. Model Studies

At present, a true mantle convection model does not exist. The combination of macroscale problems (essentially, the high degree of non-linearity) and microscale problems (the great number of plausibly significant effects) makes all modeling to date piecemeal. The problem which has been most thoroughly studied is simple Bernard convection; i.e., equations 3 - 4 simplified to

$$\left.\begin{aligned} 0 &= -\nabla\delta p + \underset{\sim}{\lambda}\,Ra\,\delta T + \nabla^2\underset{\sim}{v} \\ \dot{T} + \underset{\sim}{v}\cdot\nabla T &= \nabla^2 T \\ T(1) &= 0 \\ T(0) &= 1 \end{aligned}\right\} \quad (6),$$

This has been solved analytically up to about $Ra \simeq 10^5$ (IBID) and numerically up to $Ra \simeq 10^7$ (MCKENZIE ET AL 1973). The conclusions are that as Ra increases, rolls remain stable but cells are smaller and plumes and boundary layers become narrower.

Partial models related to understanding mantle convection can be grouped into about five classes, in accordance with their limitations.

(1) Analytic expansions at moderate Ra (MALKUS & VERONIS 1958; BUSSE 1967; RICHTER 1973). These expansions are in terms of one to three small parameters, such as $(Ra - Ra_{cr})/Ra$. Linear dependencies of properties on temperature, contained heat sources, phase transitions, and two component effects have been analysed in plane layers, and some in spherical geometry. Some results suggestive for application at still higher Ra are :
   (a) the persistence of flow planforms as Ra is increased;
   (b) the breakdown of the flow into three-dimensional patterns with internal heat sources or temperature dependent properties; and
   (c) the correspondence of steady state flow to maximization of heat transport.

(2) Two dimensional numerical integration (IBID; TORRANCE & TURCOTTE 1971; ANDREWS 1972; MCKENZIE ET AL 1973). The computer is the obvious device for higher Ra. However, the capacity and speed of present-day computers makes a full three-dimensional integration too expensive. A variety of effects -- contained heat sources, exponential temperature dependence on viscosity, dissipation, etc. -- have been examined. Phase transitions enhance the rate of flow. Contained heat sources result in broad up-plumes and narrow down-plumes, while the higher order temperature of viscosity results in narrow up-plumes and broad down-plumes. Integrations combining these effects have not yet been made. Also there have been virtually no attempts to extrapolate inferences to three dimensional flow.

(3) Long wavelength analyses (MCKENZIE 1968; KAULA 1974). The spectra of the topography, gravitational potential, and plate tectonic velocities suggest that a dominant part of the flow is broad scale, appropriate for expressions in terms of spherical harmonic coefficients $C_{\ell m}(x)$, $S_{\ell m}(x)$. If we define for scalar quantities x:

$$S_\ell(x) = \sum_{n=1}^{\ell} \sum_{m=0}^{n} \{ \overline{C}^2_{nm}(x) + \overline{S}^2_{nm}(x) \} \qquad (7),$$

and for vector quantities v:

$$S_\ell(v) = \sum_{n=1}^{\ell} n(n+1) \sum_{m=0}^{n} \{ \overline{C}^2_{nm}(v_s) + \overline{S}^2_{nm}(v_s) + \overline{C}^2_{nm}(v_T) + \overline{S}^2_{nm}(v_T) \} \qquad (8),$$

where the subscript $_s$ denotes poloidal and the subscript $_T$ denotes toroidal, then the values of $S_\ell(x)/S_{36}(x)$ are:

ℓ	Topography	Potential	Velocity
2	0.48	0.65	0.64
4	0.68	0.90	0.76
6	0.81	0.95	0.85
8	0.86	0.97	0.89

However, the continental part of the topography is largely accounted for by static isostasy, while the potential spectrum ($10^{-5}\ n^{-2}$ "rule of thumb") corresponds to a white spectrum in density. Only the velocity spectrum is found to have implications for deep flow in solutions optimizing heat transfer. The observational fact of plate tectonics is the main rationale for pursuing this approach.

(4) Boundary layer or plume studies (SCHUBERT & TURCOTTE 1971; RICHTER 1973; ANDREWS 1972; References in section 6.7) . Models confined to the lithosphere and its interaction with the asthenosphere have been rather successful in explaining characteristics of certain types of features, particularly oceanic rises (ANDREWS 1972; SCLATER & FRANCHETEAU 1970; LACHENBRUCH 1973; PARKER 1973) and underthrust lithospheric zones (SCHUBERT & TURCOTTE 1971; MCKENZIE 1969; TOKSÖZ ET AL 1971; GRIGGS 1972). These models necessarily assume a level of isostasy or zero work a few hundred kilometres deep. Recent developments in understanding the phase transition dependences on water (GREEN 1973) may allow the extension of oceanic rise models to explain the topographic and gravity lows of ocean basins as a consequence of accelerations arising from a thickening lithosphere.

More speculative work in this category are models of continental break up due to contained heat

sources, and of narrow up-plumes leading to "hot spots" (MORGAN 1972; DEFFEYES 1972).

(5) Purely mechanical studies. This category comprises the response of viscous or elastic-viscous layered media to known changes in load. Post-glacial uplift studies, which yield the principal evidence that the mantle indeed flows, are the best known examples (see references in section 6.8). Because of inadequate data on the peripheral bulge zone, there are still differences by a factor of ten as to the lower mantle viscosity. Other doubts arise from the transient nature of the uplift, and from the possible importance of non-linear dependence of strain rate on stress.

Another area of study which should develop considerably in the near future is anelastic deformation in fault zones. The inability to account for Chandler wobble with elastic dislocation models suggests that anelastic flow may be the significant excitation. In this instance, the layered elastic and viscous layered medium is broken by a fault, which is loaded by motions prescribed from the kinematic plate tectonic model. The problem is to reconcile deformation patterns from models with those observed near a fault.

4. Conclusions

Current efforts applicable to mantle convection are still rather far from directly explaining the observed gravity field and plate motions. The inferences are still quite qualitative, but progress is considerable. A list in rough order of decreasing firmness and increasing speculativeness might be :

- Compositional variations are of comparable importance to thermal variations.
- Phase transitions reinforce and amplify thermal expansion and contraction
- The smallness of variations in the gravity field indicates that the driving density differences are too small to force all the return flow through a thin asthenosphere; there must be a deeper flow.
- The temperature dependence of viscosity probably leads to a fairly constant mean viscosity as a function of depth below the asthenosphere.
- Gravity anomalies tend to reflect rather shallow conditions, while plate velocities reflect deeper conditions.
- The observed plate velocities of some centimetres per year indicate a depth of flow several hundred kilometres at least, so that the dissipation (i.e., friction) is not too great.
- If thermal plumes are narrow and do not move with time, then the mantle is significantly differentiated in heat sources and composition.

Relevant to the purposes of this conference to prescribe observations of the gravity field and secular motions, the more fundamental studies of mantle convection seem to be of little help, since they are still far from explaining existing data. A lot more modeling is needed to develop the necessary insight. It can be said, however, that for the broad scale of more than a thousand km, it is virtually certain that refinement of geodetic data would not help, particularly over oceanic areas. The system is so sluggish that on this scale there can be no doubt that the relative velocities obtained from remanent magnetism prevail in an essentially steady state manner.

The areas in which more geodetic data would help are of three types.

1. Fault zones: the margins between tectonic plates, be they tensile, compressive or strike slip. Although the plates themselves must move very steadily, at the edges there is a lot of irregular jerky motion which it is desirable to understand better for scientific as well as practical reasons, such earthquake alleviation.

2. Active continental areas: regions in which a minor (less than 1%) but perceptible portion of seismic energy is released, such as the United States from the Rockies eastward, or the Tien-Shan - Baikal belt in the USSR. In such regions there may be smaller tectonic plates or incipient rifts, but the remanent magnetism is too mixed up, and the rates too slow, to get any indication of relative motion between parts of continent to the accuracy attained for oceanic areas.

3. Post glacial uplift. As mentioned earlier some ambiguity as to interpretation still exists, which could be solved by more detailed data.

5. Acknowledgments

This work is supported by NSF grant GA-10963. This paper is Institute of Geophysics & Planetary Physics Publication No. 1233.

6. References

For each of several subject areas some references are suggested. The list is not intended to be complete or representative.

6.1 Rheology of Mantle Materials

STOCKER, R.L. & ASHBY, M.F. 1973. On the Rheology of the Upper Mantle. *Revs.geophys.space phys.* 11,391-426.

WEERTMAN, J. 1970. The Creep Strength of the Earth's Mantle. *Revs.geophys.space phys.* 8,145-168.

6.2 Compositional Considerations

CLARK, S.P.,Jr. & RINGWOOD, A.E. 1964. Density Distribution and Constitution of the Mantle. *Revs.geophys.* 2,35-88.

DICKINSON, W.R. & LUTH, W.C. 1971. A Model for Plate Tectonic Evolution of Mantle Layers. *Science* 174,400-404.

GAST, P.W. 1972. The Chemical Composition of the Earth, the Moon, and Chondritic Meteorites. In (ROBERTSON, E.C. ed.) *The Nature of the Solid Earth.* McGraw-Hill, New York,19-40.

GREEN, D.H. 1973. Contrasted Melting Relations in a Pyrolite Upper Mantle Under Mid-Oceanic Ridge, Stable Crust, and Island Arc Environments. *Tectonophysics* 17,285-297.

WYLLIE, P.J. 1973. Experimental Petrology and Global Tectonics - a Preview. *Tectonophysics* 17, 189-209.

6.3 Fundamental Stability Analyses

BACKUS, G.E. 1955. On the Application of Eigenfunction Expansions to the Problem of the Thermal Instability of a Fluid Sphere Heated Within. *Phil.Mag.Ser.7* 46,1310-1327.

CHANDRASEKHAR, S. 1961. *Hydrodynamic and Hydromagnetic Stability.* Clarendon Press,Oxford,652 pp.

JEFFREYS, H. & BLAND, M.E.M. 1951. The Instability of a Fluid Sphere Heated Within. *Mon.Not.R. astr.Soc.,geophys.Suppl.*6,148-158.

SCHUBERT, G. & TURCOTTE, D.L. 1971. Phase Changes and Mantle Convection. *J.geophys.Res.* 76, 1424-1432.

6.4 Analytical Developments at Small Rayleigh Number

BUSSE, F.H. 1967. The Stability of Finite Amplitude Cellular Convection and its Relation to an Extremum Principle. *J. fluid mech.* 30,625-649.

MALKUS, W.V.R. & VERONIS, G. 1958. Finite Amplitude Cellular Convection. *J.fluid mech.* 4,225-260.

RICHTER, F.M. 1973. Dynamical Models for Sea Floor Spreading. *Revs.geophys.space phys.*11,223-287.

6.5 Numerical Integrations in Two Dimensions

The last reference in section 6.4 plus

ANDREWS, D.J. 1972. Numerical Simulation of Sea-Floor Spreading. *J.geophys.Res.* 77,6470-6481.

MCKENZIE, D.P., ROBERTS, J. & WEISS, N. 1973. Numerical Models of Convection in the Earth's Mantle. *Tectonophysics* 19,89-103.

TORRANCE, K.E. & TURCOTTE, D.L. 1971. Structure of Convection Cells in the Mantle. *J.geophys.Res.* 76,1154-1161.

6.6 Long Wavelength Analyses

KAULA, W.M. 1974. Thermal Convection in a Sphere as an Inverse Problem, with Applications to the Earth and Moon. *J.geophys.Res.* 79 (in press).

MCKENZIE, D.P. 1968. The Influence of the Boundary Conditions and the Rotation on Convection in the Earth's Mantle. *Geophys.J.R.astr.Soc.* 15,457-500.

6.7 Boundary Layer and Plume Computations and Speculations

The last reference in sections 6.3 and 6.4, the first reference in section 6.5, plus

DEFFEYES, K.S. 1972. Plume Convection with an Upper Mantle Temperature Inversion. *Nature* 240, 539-544.

GRIGGS, D.T. 1972. The Sinking Lithosphere and the Focal Mechanism of Deep Earthquakes . In (ROBERTSON, E.C. ed.) *The Nature of the Solid Earth.* New York,361-384.

JACOBY, W.R. 1970. Instability in the Upper Mantle and Global Plate Movements. *J.geophys.Res.* 75, 5671-5680.

KAULA, W.M. 1972. Global Gravity and Mantle Convection. *Tectonophysics* 13,341-359.

LACHENBRUCH, A.H. 1973. Differentiation and the Gravitational Driving Force for Material Rising at an Ocean Ridge. *J.geophys.Res.* 78,825-831.

MCKENZIE, D.P. 1969. Speculations on the Consequences and Causes of Plate Motions. *Geophys.J.R. astr.Soc.* 18,1-32.

MORGAN, J.W. 1972. Plate Motion and Deep Mantle Convection. *Mem.geol.Soc.Am.* 132,7-22.

PARKER, R.L. 1973. Thermal Model of Ocean Ridges. *Nature phys.science* 242,137-139.

SCLATER, J.G. & FRANCHETEAU, J. 1970. The Implications of Terrestrial Heat Flow Observations on Current Tectonic and Geochemical Models of Crust and Upper Mantle on the Earth. *Geophys.J.R.astr.Soc.* 20,493-509.

TOKSÖZ, M.N., MINEAR, J.W. & JULIAN, B.R. 1971. Temperature Field and Geophysical Effects of a Downgoing Slab. *J.geophys.Res.* 76,1113-1138.

TURCOTTE, D.L. & OXBURGH, E.R. 1967. Finite Amplitude Convection Cells and Continental Drift. *J.fluid.mech.* 28,29-42.

6.8 Post-Glacial Rebound Analyses

CATHLES, L.M. 1971. Lower Mantle Viscosity Inferred from Post Glacial Adjustment of the Ocean Basins and Canada. *EOS Trans.Am.geophys.U.* 52,353.

MCCONNELL, R.K.,Jr. 1968. Viscosity of the Mantle from Relaxation Time Spectra of Isostatic Adjustment. *J.geophys.Res.* 73,7089-7105.

O'CONNELL, R.M. 1971. Pleistocene Glaciation and the Viscosity of the Lower Mantle. *Geophys.J.R. astr.Soc.* 23,299-327.

WALCOTT, R.I. 1973. Structure of the Earth from Glacio-Isostatic Rebound. *Ann.Rev.Earth plan. Sci.* 1,15-37.

7. Discussion

HOLDAHL: Do you think that VLBI and lunar laser ranging measurements will help improve the value for the drift rates?

KAULA: The remanent magnetism has a resolution of roughly 10^5 years. That is the time in which the distance the plate moves is about the same as the depth of the ocean. It is about a third of the average time between reversals. Because the driving forces are shifted only by the convection underlying the plate motion, it is plausible that the spatial average plate motion this year or any other year, will be close to the temporal average over 10^5 years. You will not find geophysicists asking for the measurement of continental drift. You will find geophysicists asking for measurement of relative motion in confused areas like the San Andreas fault region in California. This is the sort of situation to which geodetic measurements can contribute. Somewhere between the 5000 km scale of major plates and the few km scale on which marked relative motion on faults occur, *variations* in relative motion of say a centimetre per year occur. 1000 km seems to be a conservative upper limit.

MUELLER: Are you saying that the separation of VLBI stations over several thousand km is not useful anymore from the geophysicists' point of view to determine plate motion?

KAULA: Suppose you detected differences from the remanent magnetism motion between, say, stations in Hawaii and Japan. It would be a moot point whether this result reflected local or regional effects in Hawaii or Japan or both, and not motions of the entire plates.

GUBBAY: The VLBI measurement should be across a minimum distance, say a fault. This is because the maintenance of the accuracy may be bedevilled by Earth tides of much larger amplitudes. If the stations are in the same local region, this effect will be minimized.

KAULA: Of course, the experiment is better if the error sources are isolated. But you also want to measure something significant. Several hundred km baselines are desirable. If you have portable VLBI, you have a series of stations which you move along.

DUNN: You mention that the relative motion of the plates across the San Andreas fault is about 5 cm per year. Can you give a sigma on that?

KAULA: The figure of 5.5 cm per year has a sigma of 0.4 cm per year. It refers to the average motion of the entire Pacific plate with respect to the North American. I think you are referring to geodetic measurement in the region of the fault zone. This is 3.2 cm per year north at Hollister on the San Andreas, but varies elsewhere.

WHITTEN: That sounds a reasonable number. In some places it is 6 cm per year and in others it is 3 cm per year. There are places where it is locked. Back from the fault there is strain accumulation.

WALCOTT: The lithosphere is a low pass filter and we have considerable information of short wavelength (less than 5000 km) on lower mantle behaviour. What we are really lacking is long wavelength information (> 6000 km) and the only way we can get this is by studying loading on scales such as the Pacific ocean. My own personal feeling is that the data is available; you can go out and get it.

KAULA: You mean shore line features ... ?

WALCOTT: Yes; I mean sea level changes with time.

DOOLEY, J.C.
Bureau of Mineral Resources
Canberra ACT 2600
AUSTRALIA

Proc.Symposium on Earth's Gravitational Field & Secular Variations in Position (1973),248-260.

THE GRAVITY ANOMALIES OF CENTRAL AUSTRALIA AND THEIR SIGNIFICANCE FOR LONG-TERM TECTONIC MOVEMENTS*

ABSTRACT

The Bouguer gravity map of Australia shows five prominent elongated negative anomalies striking approximately east-west with peak-to-peak distances of about 80 km and amplitudes up to 160 mGal. These anomalies correlate approximately with the Officer Basin, the southern and northern parts of the Amadeus Basin, the Ngalia Basin, and the Lander Trough in the Wiso Basin. The anomalies are too large to be explained by the sediments in these basins alone, and imply substantial density variations at a depth near the crust/mantle boundary. The absence of any evidence of major tectonic activity since the Carboniferous suggests that these anomalies have existed more or less in their present form for some hundreds of millions of years. This implies that the lithosphere in this region has a long-term strength of about 100 to 200 bar.

Over this area, whose dimensions are about 10° to 15°, the average free-air anomaly is negative, with a minimum of about -30 mGal. This could arise from erosion of about 0.3 km of sediments without corresponding isostatic compensation; a time lag of intracratonic isostatic readjustment of the order of 5×10^7 years, and a lithospheric strength of one or two kbar over this time, would be implied. This anomaly may be partly associated with the deeper mantle structure as revealed by studies of satellite orbits.

On the basis of seismicity evidence some authors have proposed that the Australian continent is rifting apart. There is a well defined seismic zone running northwards from Spencer Gulf in South Australia to about latitude 30°S, but north of this the available data are far from conclusive. One hypothesis suggests that a 'Fitzroy-Spencer lineament' has been a major zone of shearing displacement since the Precambrian; this must be ruled out as the lineament intersects the gravity anomalies discussed above, and any substantial movement along it would have caused offsets of these anomalies; no such offsets are evident.

It is suggested that the central block containing the gravity anomalies has been a stable feature at least since the late Palaeozoic, and that stresses are adjusted along zones of weakness shown by minor seismicity around the boundaries. These zones approximately coincide with lineaments truncating the gravity anomalies and the major geological features, and it is probable that movements along them may have persisted for a long time, particularly on the western boundary.

1. Text

This paper is an attempt to see what can be deduced about secular variations in position from the Earth's gravity field in the Australian region, together with some evidence from seismicity.

The preliminary Bouguer gravity map of Australia (BMR, 1973) (see also ANFILOFF & SHAW 1974 , Figure 2) shows five prominent negative gravity anomalies in Central Australia between latitudes

---

* *Record 1973/205, Bureau of Mineral Resources*

20° and 30° S approximately.

These gravity anomalies correlate with five ancient basins - from south to north, the Officer Basin, southern and northern Amadeus Basins, Ngalia Basin, and the Lander Trough in the Wiso Basin. PLUMB (1972), and also the Tectonic Map of Australia (GSA, 1971) (see also Ibid, figure 1), describe the history of this area in terms of orogenies, transitional periods, cratonisation, and platform cover deposition, from the Archaean through to the early Palaeozoic.

The depth of these basins is fairly well known from seismic and aeromagnetic work, but only about half of the gravity anomalies can be accounted for by sediments unless we assume unreasonable density values. Models by ANFILOFF & SHAW (1974), MATHUR (1973); FORMAN & SHAW (1973), have all resorted to density changes deep in the crust. The negative gravity anomalies generally overlap the outcropping basement rocks, suggesting major overthrusting. Basement outcrops generally appear as low mountain ranges between comparatively low-lying and flat sediments; thus the correspondence between Bouguer anomalies and elevation is the reverse of that expected for isostasy.

The free-air anomaly profiles along longitudes 129°E and 132°E (figure 1, after WELLMAN, in prep.) show this lack of isostasy. The surface altitudes between basins are not shown to full advantage because they are plotted from gravity station heights, which are generally sited so as to avoid peaks.

No major tectonic activity has occurred in the area since the Carboniferous (PLUMB 1972), nor is there, as far as is known, any present-day seismic activity in the area (figure 2, after DENHAM et al, in prep.). Presumably the anomalies must have originated during a period of intense tectonic activity, with compressive stress and overthrusting, and then have been frozen into the crust or lithosphere and are now supported by its strength.

An estimate of the strength needed to support these anomalies can be obtained from a simple model of McKENZIE (1967). In figure 3, the upper layer is taken as a solid resting on an asthenosphere which is effectively a liquid over the geological periods concerned. An applied load centred at C causes an elastic deformation of the crust (greatly exaggerated in the diagram). Depending on the parameters involved the maximum shear stress σ_{max} will occur either at AA' and CC', or at BB'. The free-air gravity anomaly Δg at C relative to A can also be readily calculated, and thus can be related to the maximum stress by means of the equation:

$$\sigma_{max} = \Delta g \quad f(\lambda/T),$$

where λ is the width of the deflected part of the lithosphere and T is the thickness. $f(\lambda/t)$ follows different laws according to whether σ_{max} occurs at BB' or CC'; the resulting function is plotted in figure 3.

Estimates of amplitude and wavelength of the anomalies over the five basins are listed in table 1. The Amadeus Basin was treated firstly as two separate basins, and secondly as one basin with the central gravity high smoothed out. Estimates of the shear strength scaled from figure 3 are listed for a lithosphere 40, 60, and 100 km thick.

Thus this leads to a minimum strength of the lithosphere of say 100 or 200 bars. Laboratory measurements give somewhere about 4000 bars (GRIGGS et al 1960). Naturally it is expected that strength over geological periods is much less, as stress applied for long periods causes deformation without

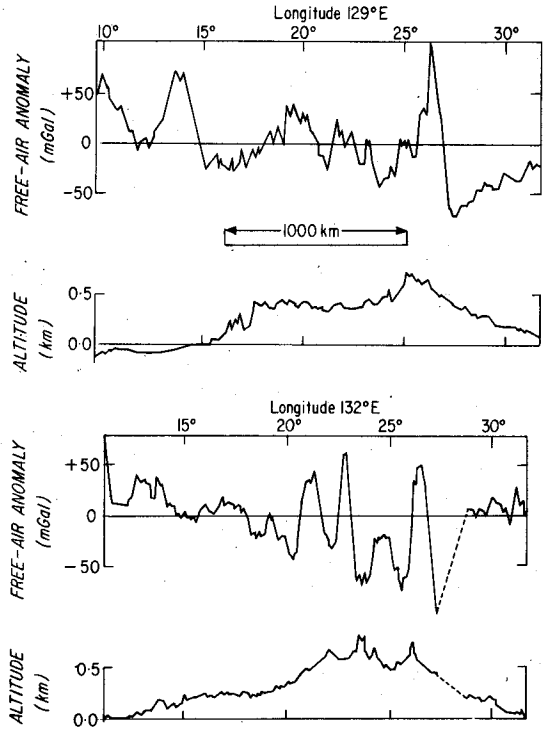

Figure 1. Gravity and Altitude Profile Across Australia

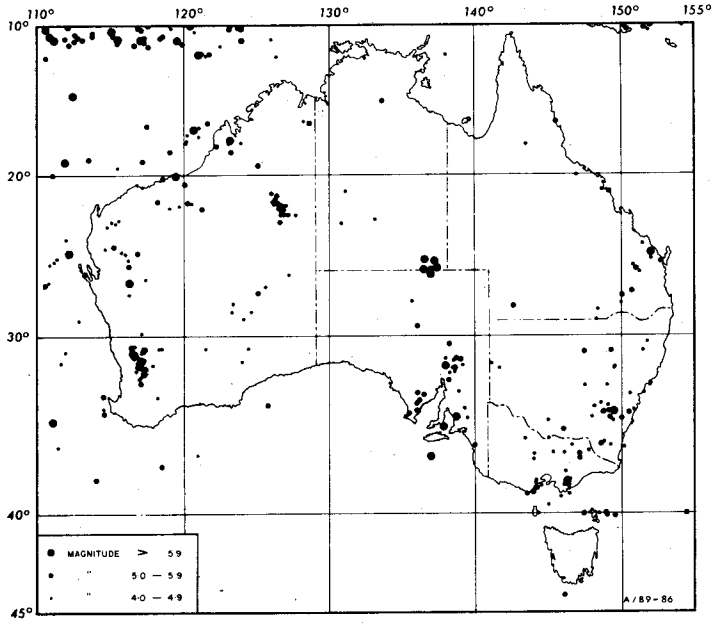

Figure 2. Australian Seismicity 1900-1972

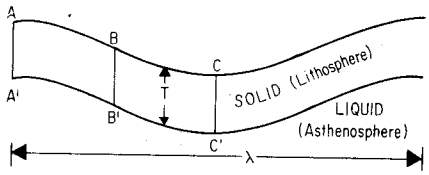

Maximum stress in bars at AA', BB', or CC'

$\sigma_{max} = \Delta g \, f(\lambda/T)$

$f(\lambda/T)$ as below

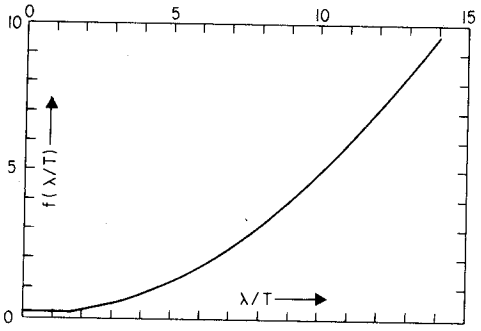

Figure 3

Table 1

Basin	Anomaly (mGal)	Width (km)	Maximum Stress T = 40 km	60 km	100 km
Officer	140	225	210	98	42
Amadeus South	105	175	95	42	21
Amadeus North	115	225	173	80	35
Amadeus (whole)	100	400	480	240	80
Ngalia	110	200	132	55	28
Lander Trough	60	250	114	54	21
Regional Anomaly (a)	30	2000	3600	1590	570
(b)	20	2000	2400	1060	380

breaking. CAREY (1954) has proposed the concept of 'rheidity', or relaxation time beyond which stresses cannot persist without viscous flow becoming important. For igneous rocks he estimates about 10^9 years. Also he defines 'practical strength', which is a function of time and is the stress which can be supported for a given period. Thus we say that the practical strength of the lithosphere in central Australia is at least 100 or 200 bars for a period of about 2×10^8 years This is consistent with CAREY's estimate of rheidity for igneous rocks.

If we examine the free-air anomaly profiles (figure 1), particularly along 132°E, we note that, if local effects of these major anomalies are smoothed out, there is a general negative value in the

central portion compared with the southern and northern ends, with a width of 1000 km or more. To study this in more detail a compilation of free-air anomalies of 1^{o} x 1^{o} lat/long 'squares' has been made for the Australian area. This is based largely on MATHER's (1969a, 1969b) figures, but includes more data recently available, some from anomalies on tape in BMR national gravity repository, some calculated by WELLMAN (in preparation) and others estimated from Bouguer anomaly maps and then corrected to the mean elevation of the square for land squares. For more recent BMR marine surveys south and west of the continent the average was estimated directly from preliminary free-air anomaly maps. With coastal squares (i.e. part marine and part land) a combination of these two methods was used.

Some of these data are in a preliminary form and should not be regarded as the best that could be derived from available data for 1^{o} x 1^{o} squares; however, if averaged over larger squares errors become much smaller. The series of maps presented here (figures 4, 5, 6 and 7) show contours for means of 3^{o}, 5^{o}, 7^{o}, and 10^{o} squares based on running averages of the 1^{o} square means.

These all show a persistent gravity low in central Australia.

Consider an infinite slab of density anomaly $\Delta\rho$ and thickness T; the gravitational attraction is $\overline{g} = 2\pi\ k\ \Delta\rho\ T$. If the slab has finite width, then by calculating the integrated anomaly of a simple step fault we find that by averaging over a slab of width about 10T we get about $0.9\overline{g}$, the remaining $0.1\overline{g}$ being in the 'tails' of the anomaly.

Similarly, if we consider that the Earth is homogeneous below a depth T, the average excess pressure on a level surface at depth L below this slab is $g_o \Delta\rho T$, where g_o is the surface gravity (actual variation with depth being very small near the surface). The gravity anomaly of such a slab is approximately proportional to the anomalous stress on a level surface beneath it.

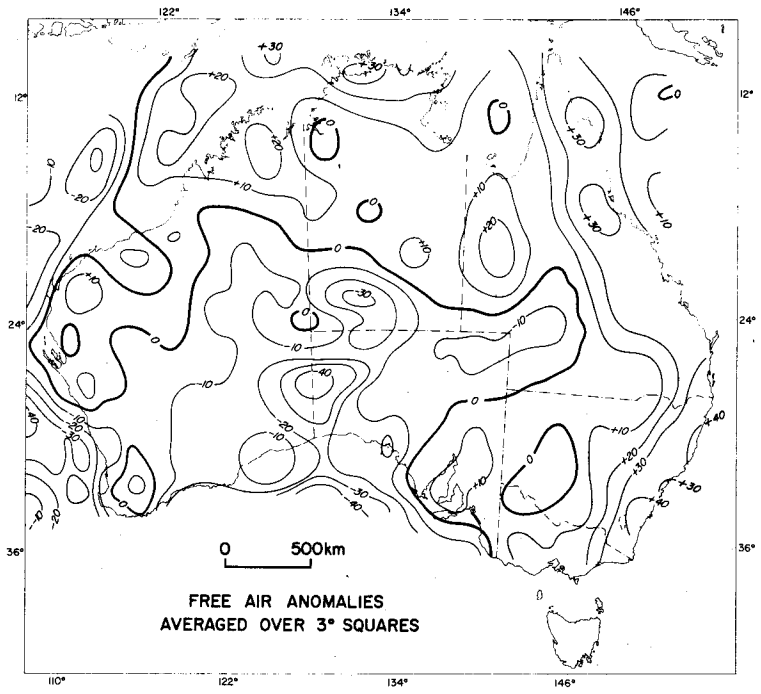

Figure 4.

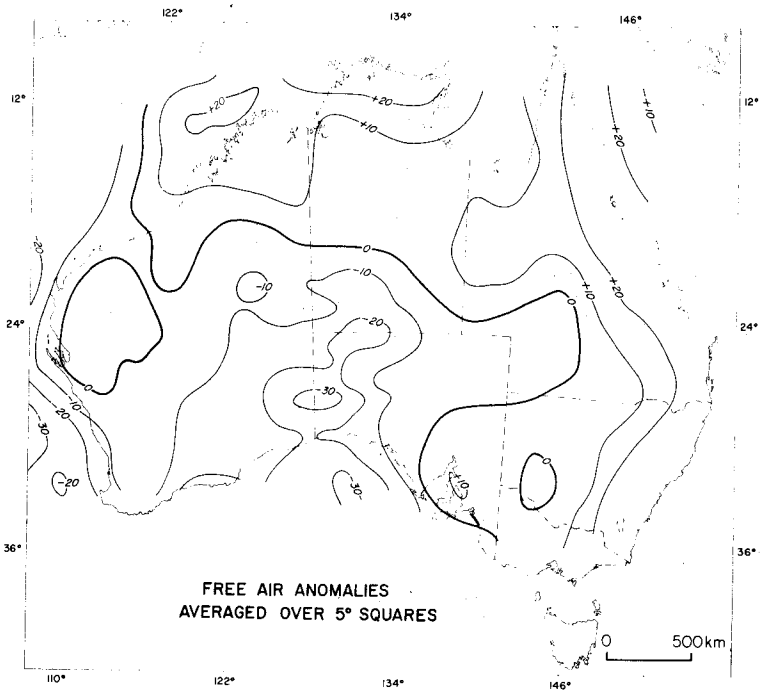

Figure 5.

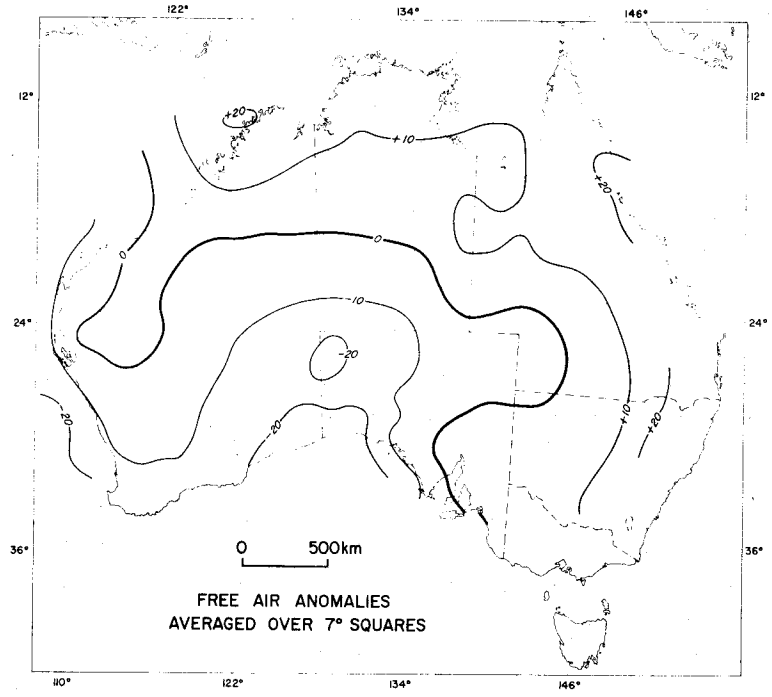

Figure 6.

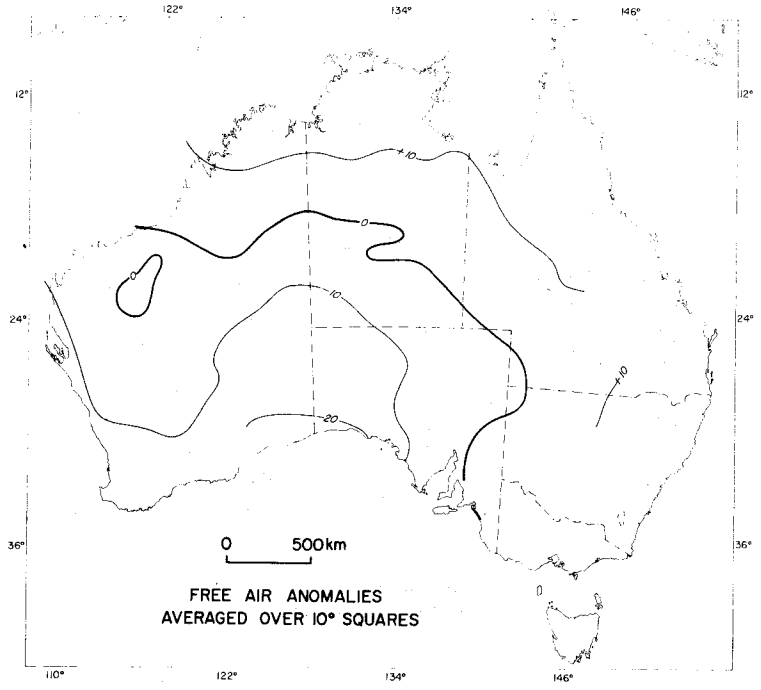

Figure 7

WELLMAN (in preparation) has concluded from Fourier analysis that there is very little lateral density variation beneath about 60 km depth, except for the sources of the very broad anomalies in the low-order spherical harmonics of the Earth's field, as shown for example by satellite orbits. If we neglect these and assume that the whole anomaly is associated with sources in the upper 60 km, then horizontal averages over 600 km, or about 5°, would represent the stress at or just below this depth, and give an indication of strength. This gives a figure of say 1600 bars.

If part of the anomaly is due to much deeper sources, then the strength at great depth needs to be of this order. Assume all of the anomaly is caused by density variations below the surface at depth L; then for the slab, ρ and T are constant, and $\frac{\Delta(g\rho T)}{g\rho T}$ is the order of $\frac{\Delta g}{g}$, or about 1 in 10^4 and can be neglected.

Thus we need to separate anomaly sources about 60 km from deeper, presumably much deeper, sources. This is the old problem of separating residual and regional, and of course there is no unique way of doing this.

As one possible approach to this problem, the satellite harmonic field of 2-16th order was used as a regional (figure 8, from figure 1 of ANDERSON et al 1973) based on data of GAPOSCHKIN & LAMBECK (1971). This is based purely on satellites - published fields based on combination of satellite and terrestrial data use part of the Australian data but not all, and hence are likely to introduce bias in different areas. The 16th-order harmonics have a wavelength of about $22\frac{1}{2}^{\circ}$; thus this probably represents effects from about 300 km depth or more. The residual derived from 5° means minus 2-16th order satellite field is shown in figure 9. We can still see an anomaly of say -20 mGal and about 2000 km wavelength; this gives a strength of, for T = 100 km, 380 bars; for T = 60, 1060 bars.

Elsewhere, (DOOLEY 1973) I have suggested that this anomaly could be due to slow erosion of the higher parts of the shield, with a long time constant in the process of isostatic compensation. The rate of

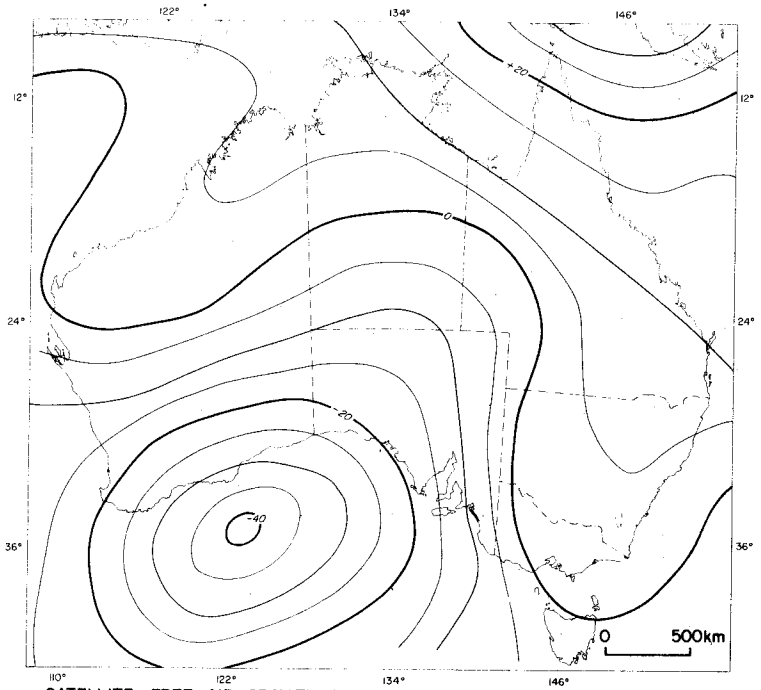

Figure 8

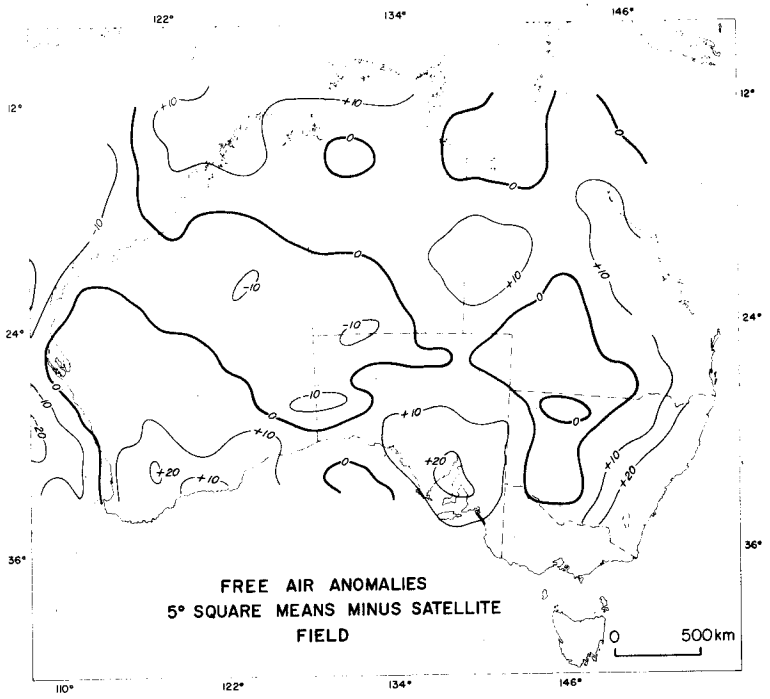

Figure 9

erosion was estimated at something of the order of 10^{-5} m/yr. Erosion without compensation of 1 km of sediments would produce a negative anomaly of about 100 mGal ($41.85\rho_s$, where ρ_s is the density of the material removed), so the anomaly estimated above of 20-30 mGal would imply a time-lag of isostatic compensation of about 20-30 M.y., and the lithospheric strength of the order of 1 kbar estimated above would be the effective strength for this period. Note the great difference in time of isostatic adjustment from that estimated from the Fennoscandian shield post-alluvial rebound of about 15 000 yr. The latter is usually regarded as referring to upper mantle rheidity. If my conclusions are correct and give representative strengths and time constants for shield lithospheres, it may be that the shields move fairly rapidly into a position of isostatic equilibrium as a whole, while maintaining intra-shield stress differences in the lithosphere for much longer periods of time.

We note in passing that LAMBECK (1972) has estimated that the harmonics of order as low as 8 or 9 could be supported in the lithosphere with a strength of 1500 bars.

The relation between earthquake magnitude and stress is anything but precise, but the available data suggest that earthquakes of magnitude M_s = 7 or 8 would be associated with stresses of the order of 1000 bar.

The seismicity map of Australia (DENHAM et al, in preparation) is shown in Figure 4. It must be borne in mind that the distribution of earthquakes shown is affected by density of population and instrumentation; the distribution can probably be regarded as fairly unbiased by these factors for magnitudes greater than 5. As Australian seismicity is low, this does not leave much data for statistical generalisation. In fact, in several cases, one earthquake and its aftershocks have changed the picture entirely.

As regards central Australia, there is a well defined seismic zone running northwards from Adelaide to about 30°S, fairly large recent earthquakes in the Simpson Desert (STEWART & DENHAM 1974) and Canning Basin (DENHAM et al, in preparation), and a few minor events.

Several authors have proposed that the Australian continent is rifting or shearing along a plate boundary through the centre. Figure 10 shows three proposed lineaments - that of COOK (1966; 1971), which initially was based partly on gravity evidence; that of CLEARY & SIMPSON (1971) based on seismicity and a proposed relation to a displacement of the Southern Ocean mid-ocean ridge south of Adelaide; and that of STEWART & MOUNT (1972) who describe the 'Fitzroy-Spencer lineament' on the basis mainly of seismicity.

Cook's proposed lineament was based on correlation of widely separated gravity anomalies across areas where few or no observations were available at the time. Subsequent surveys have made these correlations improbable.

STEWART & MOUNT postulate that the Fitzroy-Spencer lineament has been a zone of shearing relative movement between two blocks of the continent since Precambrian times. However, we note that their lineament intersects at an angle the major gravity anomalies in central Australia. If indeed shearing movement had continued for a prolonged geological period, then we would expect it to show in a large offset displacement of these gravity anomalies, since we have shown that they are some hundreds of millions of years old. Examination of the gravity map shows no indication of such displacement. The same could be said for the major geological boundaries of the associated basins and blocks.

CLEARY & SIMPSON's proposed zone cannot be dismissed on these grounds, as it skirts along the eastern edge of the supposed stable block and then trends westwards along the length of the Ngalia Basin.

However, in view of the low seismicity it seems premature to draw any firm conclusions about trans-continental zones of activity. The central block which we have studied above appears to have shown little or no seismicity for the period for which data are available, but there is a suggestion that earthquakes tend to occur around its edges. In view of the figures for the lithospheric strength inferred above for the central block, it seems that this may be a comparatively strong and stable slab surrounded by weaker material, or zones of weakness, in which stress adjustments are occurring.

Moreover, recent studies of earthquake first motions by DENHAM (pers.comm.) suggest different stress regimes - north-south compression in south-eastern Australia, and NE-SW compression in the north-western part of the continent.

ANFILOFF & SHAW (1974, figure 2) have drawn attention to a NNE trending lineament which truncates the major gravity anomalies on the western side, and which also truncates the major geological features - the Arunta and Musgrave blocks, and the Officer, Amadeus, and Ngalia Basins. The zone of seismicity forming the western boundary of the stable block proposed above is approximately linear and coincides approximately with ANFILOFF & SHAW's lineament. Thus it appears that movement may still be taking place along or close to this lineament, which is apparently of ancient origin; the time of commencement of these movements is difficult to estimate.

Further, ANFILOFF & SHAW postulate a south-east trending lineament truncating the northern gravity anomalies and geological features of the block (IBID, figure 10). The Simpson Desert earthquakes occurred somewhat to the east of this lineament. Examination of the gravity (BMR 1973) and tectonic (GSA 1971) maps show that it would be reasonable to move the line of truncation eastwards so as to pass through these earthquakes. The seismicity zone southwards from here shows some agreement with the trend of the eastern boundary of the gravity anomalies and geological features; however, both the boundaries and the seismicity zone are irregular in shape, and this boundary cannot be defined clearly.

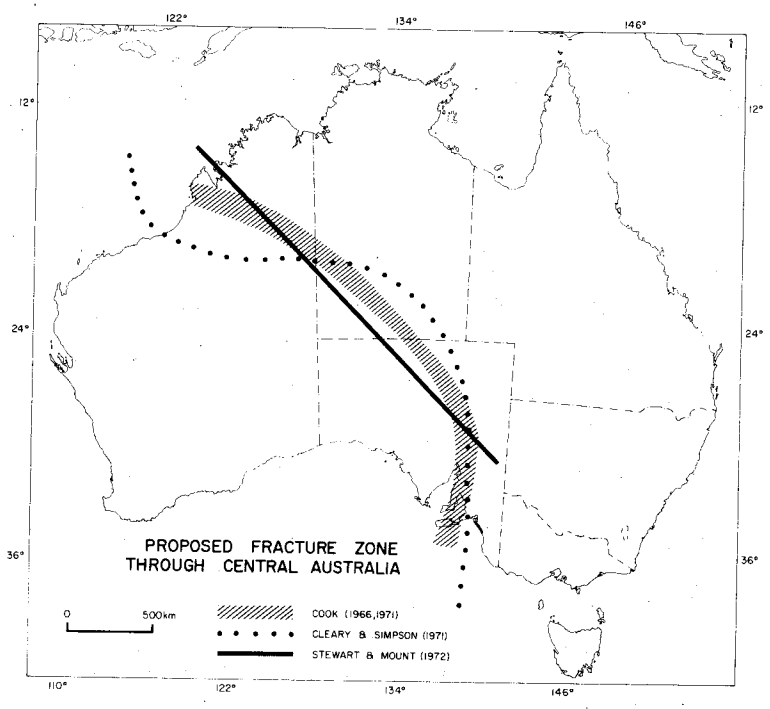

Figure 10

2. Conclusions

1) The largest gravity anomalies in the shield area are not associated with evidence of seismicity. This is distinct from the situation in island arcs.

2) These anomalies are very old and imply a significant long-term strength of the shield lithosphere.

3) The lack of noticeable displacement of the anomalies along the proposed Fitzroy-Spencer lineament precludes any significant long-term strike-slip motion along this lineament.

4) Much more seismicity data are required to enable reliable confirmation or rejection of proposed trans-continental rupture zones.

5) Four lines of evidence, i.e. truncation of gravity anomalies, truncation of geological features, the estimated strength of the central block, and the seismicity zones, suggest that the central block has been a stable feature since late Palaeozoic (or possibly earlier) and that

stresses in the continental plate have been relieved by movements along the boundaries of this block throughout a considerable period of geological time.

3. Acknowledgment

The permission of the Director, Bureau of Mineral Resources, Australia, to publish this paper is acknowledged.

4. References

ANDERSON, R.N., McKENZIE, D.P. & SCLATER, G.P. 1973. Gravity, bathymetry and convection in the Earth. *Earth plan. Sci.Letters.* 18, 391.

ANFILOFF, W. & SHAW, R.D. 1974. The gravity effects of two large uplifted granulite blocks in separate Australian shield areas. (This volume,273-289).

BMR 1973. Preliminary Bouguer Anomalies, Australia, scale 1:5 000 000. Government Printer, Canberra.

CAREY, S.W. 1954. The rheid concept in geotectonics. *J. geol.Soc.Aust.* 1, 67.

CLEARY, J.R. & SIMPSON, D.W. 1971. Seismotectonics of the Australian continent. *Nature.* 230, 239.

COOK, P.J. 1966. The Illamurta structure, central Australia: its development and relationship to a major fracture zone. *Bur.Miner.Resour.Aust.Rec.* 1966/46 (unpublished).

COOK, P.J. 1971. Illamurta diapiric complex and its position on an important central Australian structural zone. *Bull.Amer.Ass.petrol.Geol.* 55, 64.

DENHAM, D., EVERINGHAM, I.B. & GREGSON, P.J. East Canning Basin Earthquake, March 1970. (In preparation).

DENHAM, D., SIMPSON, D.W., GREGSON, P.J. & SUTTON, D.J. 1972. Travel times and amplitudes from explosions in Northern Australia. *Geophys.J.* 28, 225.

DOOLEY, J.C. 1973. Is the Earth Expanding? *Search.* 4, 9.

FORMAN, D.J. & SHAW, R.D. 1973. Deformation of the crust and mantle in central Australia. *Bur.Miner.Resour.Aust.Bull.* 144.

GAPOSCHKIN, E.M. & LAMBECK, K. 1971. Earth's gravity fields to 16th degree and station co-ordinates from satellites and terrestrial data. *J.geophys.Res.* 76. 4855.

GRIGGS, D.T., TURNER, F.J. & HEARD, H.C. 1960. Deformation of rocks at 500 to 800°C. *Geol.Soc.Amer.Mem.* 79, Chap.4.

GSA. 1971. Tectonic Map of Australia, 1971. *Geol.Soc.Aust.* Sydney.

LAMBECK, K. 1972. Gravity anomalies over ocean ridges. *Geophys.J.R.astron.Soc.*30, 37.

McKENZIE, D.P. 1967. Some remarks on heat flow and gravity anomalies. *J.geophys.Res.* 72, 6261.

MATHER, R.S. 1969a. The free air geoid for Australia. *Geophys.J.R.astron.Soc.* 18, 499.

MATHER, R.S. 1969b. The free air geoid for Australia from gravity data available in 1968. *Unisurv.Rep.* University of New South Wales, Sydney.

MATHUR, S.P. A proposal for a deep seismic sounding survey in central Australia. *Bur.Miner. Resour.Aust.Rec.* (in preparation).

PLUMB, K.A. 1972. Tectonic evolution of Australia, summary. *Bur.Miner.Resour.Aust.Rec.* 1972/37 (unpublished).

STEWART, I.C.F. & DENHAM, D. 1974. Simpson Desert earthquake, central Australia, August 1972. *Geophys.J.R.astron.Soc.* (in press).

STEWART, I.C.F. & MOUNT, T.J. 1972. Earthquake mechanisms in South Australia in relation to plate tectonics. *J.geol.Soc.Aust.* 19, 41.

WELLMAN, P. Australian gravity and altitude spectra. (In preparation).

5. Discussion

KAULA: Is there any evidence of a low-velocity layer under Australia? If so, what is the depth to the top of this layer?

DOOLEY: DENHAM ET AL (1972), as a result of refraction recordings from large explosions in the Ord River area, have found indications of a low-velocity layer with a lower boundary of about 160 km depth. The thickness of the zone could not be determined.

PURINS*: To what extent has a study of the Earth's density distribution been carried out in Australia and what are the future plans?

DOOLEY: WELLMAN (in.prep.) has modelled the free air gravity field in Australia in terms of average density and thickness of $2^\circ \times 2^\circ$ crustal blocks on the assumption that each such block is isostatically compensated.

A computer-based file is being established in the Bureau of Mineral Resources (Canberra) for density measurements of bore cores and rock specimens; however no comprehensive analysis has yet been made of these data.

* Written Question.

JOHNSON, B. D.
LEE, T. J.
School of Earth Sciences
Macquarie University
North Ryde NSW 2113
AUSTRALIA

Proc. Symposium on Earth's Gravitational Field & Secular Variations in Position (1973), 261-272.

A RAPID METHOD FOR THE COMPUTATION OF THE GRAVITATIONAL ANOMALY DUE TO COMPLEX THREE DIMENSIONAL STRUCTURES

ABSTRACT

A rapid method for the evaluation of the gravity field over complex structures can be developed by representing the structure as a sum of cubic elements of side a and density ρ.

The vertical component of the gravitational attraction for each cubic element is calculated from

$$g_z = G\rho \left[\frac{a^3 z}{R^3} + \frac{7}{96} \frac{a^7}{R^7} \left(3z - \frac{9z(x^4 + y^4 + z^4)}{R^4} + \frac{4z^3}{R^2}\right)\right]$$

where x, y and z are the coordinates of the observation point with respect to the centre of the cube, G is the gravitational constant and $R^2 = x^2 + y^2 + z^2$. The above formula is obtained by a multipole expansion of the integral expression for the potential of a cube, neglecting terms above order 4, and is valid when the required accuracy A_4 is less than

$$\frac{Ga^3}{R^2} \left(\frac{a\sqrt{3}}{2R}\right)^8 / \left(1 - \frac{a\sqrt{3}}{2R}\right) .$$

A further simplification may be obtained by only using the first term of the expansion when the specified accuracy, A_o, is less than

$$\frac{Ga^3}{R^2} \left(\frac{a\sqrt{3}}{2R}\right)^4 / \left(1 - \frac{a\sqrt{3}}{2R}\right)$$

The exact expression for the cube is only used in the restricted region close to the cube.

An array of attraction values for the cube is calculated once for each level in the model and then convoluted with an observation array. The convolution is limited by the lateral extent of the model at that level. Density variations within the model require the attraction array to be multiplied by a constant value when changing from one density region to another.

The ability to specify the required accuracy enables extremely rapid preliminary calculations to be performed. A final calculation can be carried out using a greater accuracy when the model is deemed to be correct.

1. Introduction

Several methods exist in the literature for the computation of the gravitational attraction of three-dimensional models. The methods vary greatly in the complexity of the models, the speed of calculation and in the resulting accuracy.

The most widely used method is that of TALWANI & EWING (1960) in which the model is divided into horizontal polygonal laminae the attractions of which are summed at each observation point. The amount of work involved is the product of the number of stations, the number of laminae, and the

number of faces on each lamina. The resulting calculations are relatively rapid and accurate, however, it is difficult to change the model easily unless the polygonal laminae form parts of vertical prisms.

A more rapid method which is based on vertical prisms is that of BOTT (1959) who replaces prisms by a line mass approximation. This is shown to be accurate at a great enough distance from the prisms, figure 2, but leaves us with the problem of calculating the points nearest to the model. The amount of work involved is the product of the number of prisms and the number of stations.

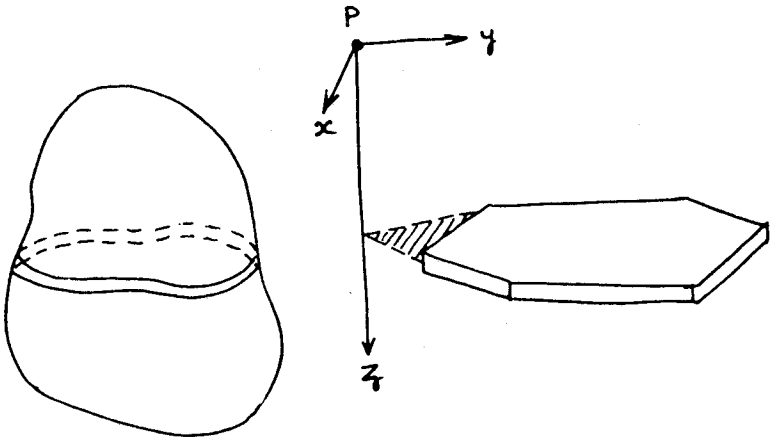

Figure 1. Principle of Lamina Method
Attraction at P due to shaded area

$$g_z = G\rho \left| \tan^{-1} \left\{ \frac{z(by - az^2)}{x\left[(1 + a^2)z^2 + b^2\right] - (a^2z^2 + b^2)\sqrt{x^2 + y^2 + z^2}} \right\} \right|_{x_{k+1},\, y_{k+1}}^{x_k,\, y_k}$$

where $a = \dfrac{x_{k+1} - x_k}{y_{k+1} - y_k}$ $\qquad$ $b = \dfrac{x_k y_{k+1} - x_{k+1} y_k}{y_{k+1} - y_k}$

after TALWANI & EWING (1960)

In order to overcome the accuracy problem an exact expression for the attraction of a prism was formulated by NAGY (1966), figure 3.

The expression is a result of performing a volume integration of a point mass over the prism volume

$$\Delta g_z = G\rho \int_V \frac{z\,dv}{r^3}$$

The complete expression contains 24 terms, each of which contains a logarithmic or inverse trigonometric function together with square roots.

A much neater form of the expression has been given by GOODACRE (1973) and this may be further

simplified to give

$$g_z = G\rho \left|\left|\left| \; x \ln \left\{\frac{y+r}{(x^2+z^2)^{\frac{1}{2}}}\right\} + y \ln \left\{\frac{x+r}{(y^2+z^2)^{\frac{1}{2}}}\right\} \right.\right.\right.$$

$$- z \arctan \left\{\frac{xy}{zr}\right\} \Bigg|_{x_1}^{x_2} \Bigg|_{y_1}^{y_2} \Bigg|_{z_1}^{z_2}$$

which may be written as a subroutine.

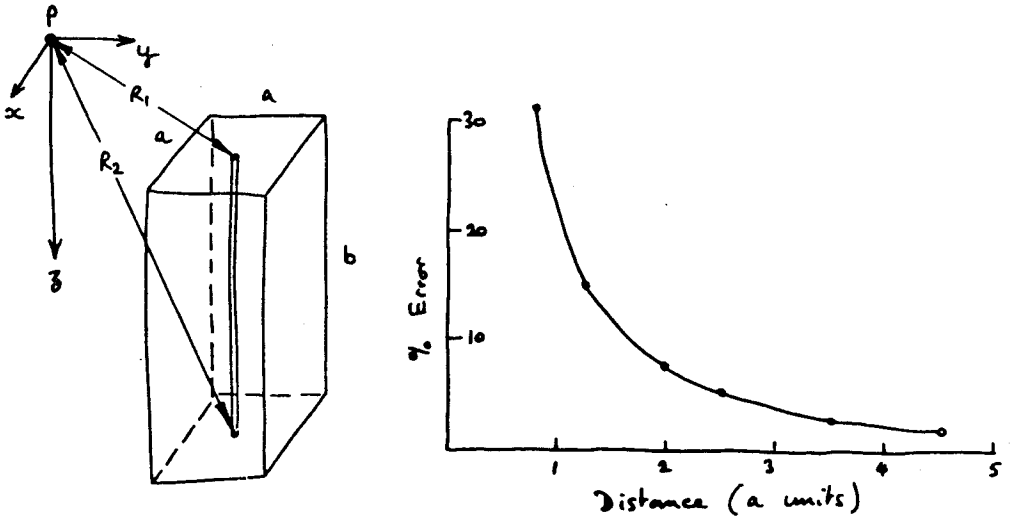

Figure 2. Principle of Line Mass Method

Attraction at P due to line mass

$$= G\rho\, a^2 \left\{\frac{1}{R_1} - \frac{1}{R_2}\right\}$$

after BOTT (1959)

The method although producing an exact solution, is very lengthy, particularly when it is noted that the evaluation is carried out for every prism and for every station.

There is therefore a considerable difference in the accuracy and speed of the various presently used methods. ST.JOHN & GREEN (1967) attempted to overcome these difficulties by using the exact formula close to the station and the line mass formula at distances removed from the station. There is, however, no provision in their method for ascertaining the accuracy of the calculations in ord to either change the formula used or to truncate the calculations.

There is therefore a choice in existing techniques between exact and slow methods and more rapid in which the calculations may be inaccurate in certain points. The aim in this paper was to devise a method in which the required accuracy determines the complexity of the calculation required at any point.

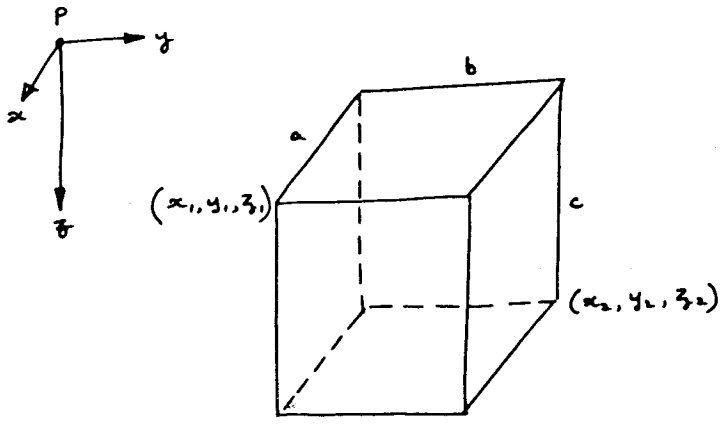

Figure 3. Principle of Prism Method.

2. Development of Approximation Formula for the Cube

The gravitational potential, U, due to an arbitrary volume v, and density ρ, may be written as

$$U = G\rho \int_v \frac{dv}{|\vec{R} - \vec{r}|} \qquad (1),$$

where G is the gravitational constant.

Expanding the reciprocal distance term as a series of Legendre functions (MACROBERT 1967, p.79) of argument cos γ, γ being defined in Figure 4,

$$U = \frac{G}{R}\rho \int_v \sum_{n=0}^{\infty} \left(\frac{r}{R}\right)^n P_n (\cos \gamma)\, dv \qquad (2).$$

We shall now restrict ourselves to the special case where the volume is a cube of dimension a and R is the distance of the observation point from the centre of the cube.

The integration can be performed by interchanging the order of integration and summation and expanding the Legendre functions by their addition formula (MACROBERT 1967, p.128).

$$\text{Thus } U = G\rho \left(\frac{a^3}{R} + \frac{7}{60} \frac{a^7}{R^9} \frac{1}{2^4} \{3R^4 - 5 (x^4 + y^4 + z^4)\} \right) \qquad (3)$$

where harmonic terms of greater than order 4 have been neglected (see Appendix).

The vertical component of the gravitational attraction due to a cube is then obtained by differentiating with respect to z, the above expression for the potential.

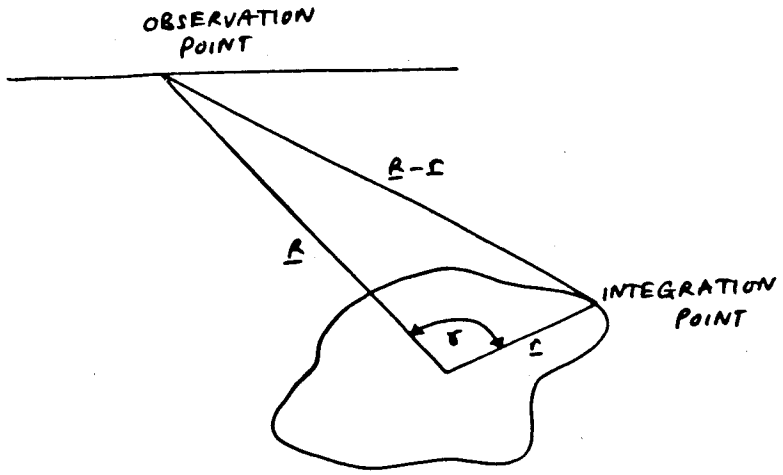

Figure 4.

$$\text{Thus } \Delta g_z = G\rho \left\{ \frac{a^3 z}{R^3} + \frac{7}{96} \frac{a^7}{R^7} \left(3z - \frac{9z(x^4+y^4+z^4)}{R^4} + \frac{4z^3}{R^2}\right)\right\} \qquad (4)$$

GRANT (1952) has shown that the remainder, A_n, satisfies the inequality

$$A_n < \frac{Ga^3\rho}{R^2} \left(\frac{a\sqrt{3}}{2R}\right)^{n+1} / \left(1 - \frac{a\sqrt{3}}{2R}\right) \qquad (5)$$

where n is the highest order of the terms included. Because of the symmetry of the cube, the terms included in equation 4 are for $n = 0$ and 4 and the first term neglected is for $n = 8$.

In equation 4, the first term in the expansion represents a sphere centred at the centre of the cube and having the same mass as the cube. The remaining terms approximate the deviation of the cube from a sphere.

In a similar problem, GRANT (ibid) used expansions of up to and including order 2 to determine the position and shape of a gravitational source.

In practice, it has been found necessary to scale the coordinates with respect to the distance R in order that computer accuracy be maintained. The working formulation for equation 4 is thus

$$\Delta g_z = G\rho z \left\{ \left(\frac{a}{R}\right)^3 + \frac{7}{96} \left(\frac{a}{R}\right)^7 \left[3 - 9\left\{\left(\frac{x}{R}\right)^4 + \left(\frac{y}{R}\right)^4 + \left(\frac{z}{R}\right)^4\right\} + 4\left(\frac{z}{R}\right)^2\right] \right\}$$

In a similar manner the exact expression has been rearranged and normalised with respect to z.

$$\Delta g_z = G\rho z \left|\left|\left| \frac{x}{z} \ln \left\{ \left(\frac{y}{z} + \frac{R}{z} \right) \Big/ \left(\frac{x^2}{z^2} + 1 \right)^{\frac{1}{2}} \right\} + \frac{y}{z} \ln \left\{ \left(\frac{x}{z} + \frac{R}{z} \right) \Big/ \left(\frac{y^2}{z^2} + 1 \right)^{\frac{1}{2}} \right\} \right.\right.\right.$$

$$\left. - \arctan \left\{ \left(\frac{x}{z} \frac{y}{z} \right) \Big/ \frac{R^2}{z^2} \right\} \right|_{x_1}^{x_2} \Big|_{y_1}^{y_2} \Big|_{z_1}^{z_2}$$

3. Application

In practice, the simple sphere calculation is sufficient for all but the closest parts of the body where the more accurate multipole expansion or the exact formulations may be required.

The required formulation is predetermined by the examination of the remainder term as calculated by equation 5 and comparing this with the required accuracy. The same remainder term may be used to truncate the calculation so that observation points beyond a certain distance are omitted.

The procedure is then to divide the model into levels of the dimension of the cube heights. An attraction array is calculated for a cube in the highest level. The calculations are performed in order with increasing distance from the centre of the cube, so that each calculation is tested against the remainder term to determine the use of the next simplest form of the calculation. This attraction array is calculated for a 45° segment since the symmetry properties of the cube allow the remaining area to be copied from the calculated segment (Figure 5).

The attraction array is then convolved with the observational array, the convolution being performed with the origin of the attraction array over the centre of each cube in the level of the model (Figure 6). Since the density may vary from one prism to another, a multiplying factor is applied to the attraction array when changing from one density to another.

The calculation proceeds by moving to the next level down in the model and computing a new attraction array and continuing as before. The calculation proceeds level-by-level until either the model is complete or the attraction array at any particular level has its maximum value below the required accuracy.

Figure 7 is a plot of the terms used in the calculation of the attraction array as a function of x, y and z being the coordinates of the observation point with respect to the centre of the cube. It can be seen that the exact expression is required only for the closest calculations and even the multipole expansion gives way to the simple sphere calculation. The distance at which the calculations are terminated is seen to decrease the size of the attraction array very rapidly and levels deeper than this distance need not be considered in the calculation. A plot of the relative times for each level is shown down the right side of the diagram.

The resulting effects of the approximation method are that the very lengthy calculations for the large numbers of blocks required for complex bodies are replaced by a relatively small number of more rapid calculations.

The present program is currently being used to calculate the topographic correction of the region around Macquarie Island, an area of over 600 km square. Initial tests on this model show that reasonably accurate results are being obtained in a time much less than for the exact methods.

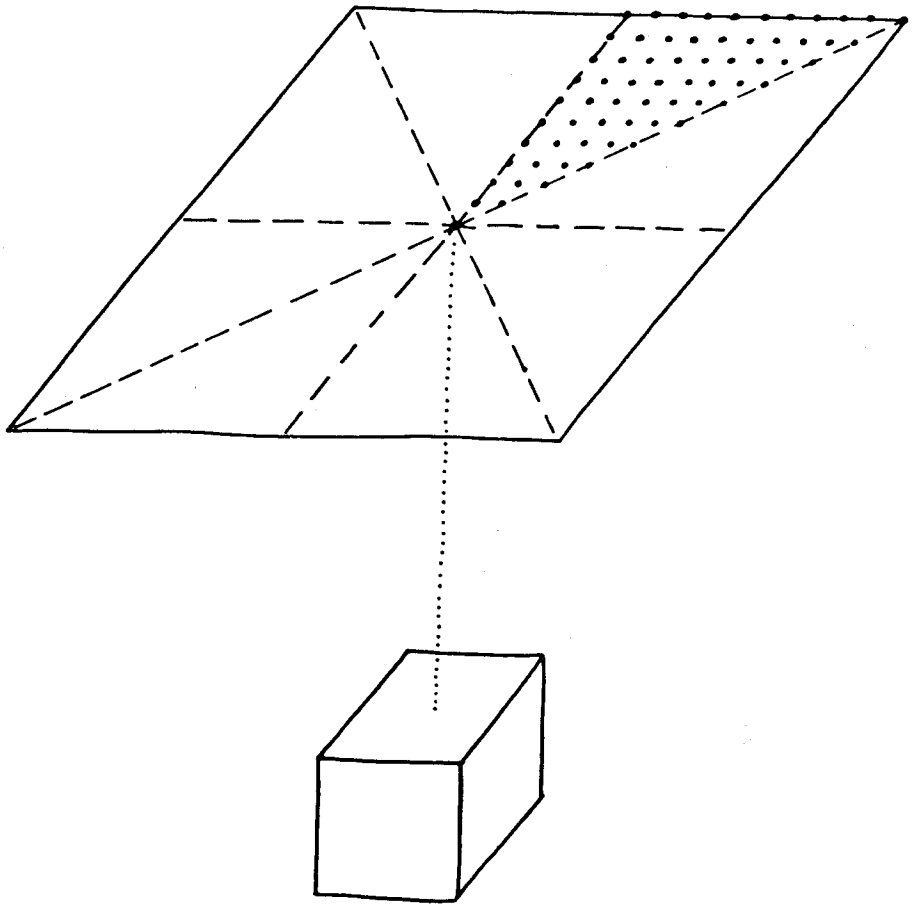

Figure 5. Calculation of Attraction Array

4. Developments

The efficiency of the program may be improved by writing the crucial part of the calculation in assembler language as there is a considerable amount of array address calculation involved. This however, makes the program machine dependent.

A correction could be easily incorporated to allow for a spherical earth distortion after the manner of TAKIN & TALWANI (1966). The restriction, that the model, the attraction array and the observation array lie on a rectilinear grid, however, restricts the model to lie within a relatively small segment of the sphere.

In some applications the computation of the magnetic field together with the gravity field is required. Similar expressions for the exact, multipole and spherical dipole magnetic attractions have been derived and will be presented elsewhere. Extra storage is required since the summation must be carried out for each of the three vector components. The resulting total field anomaly can only be calculated on completion of the model.

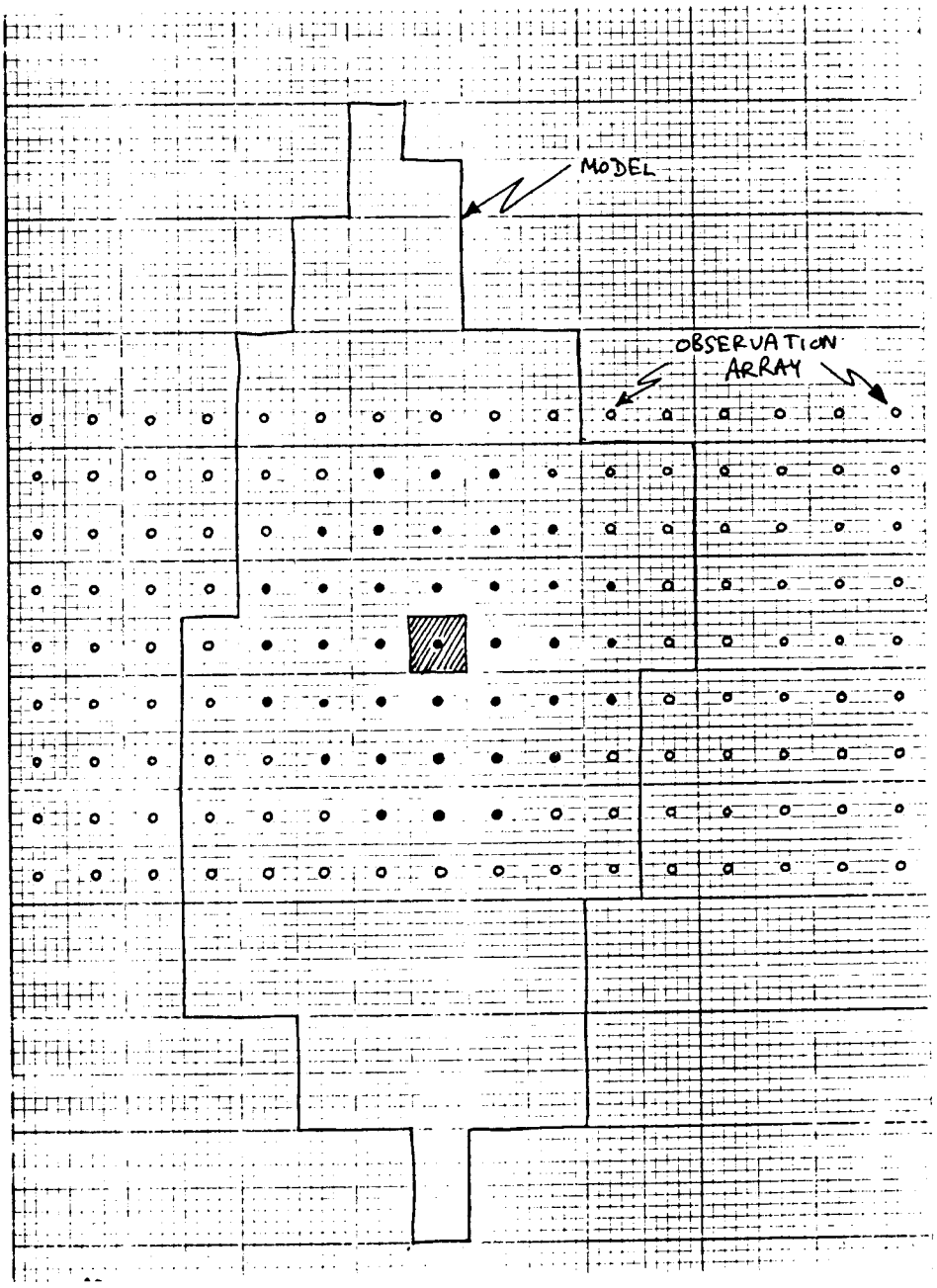

Figure 6. Addition of Attraction Due to One Cube to the Observation Array.

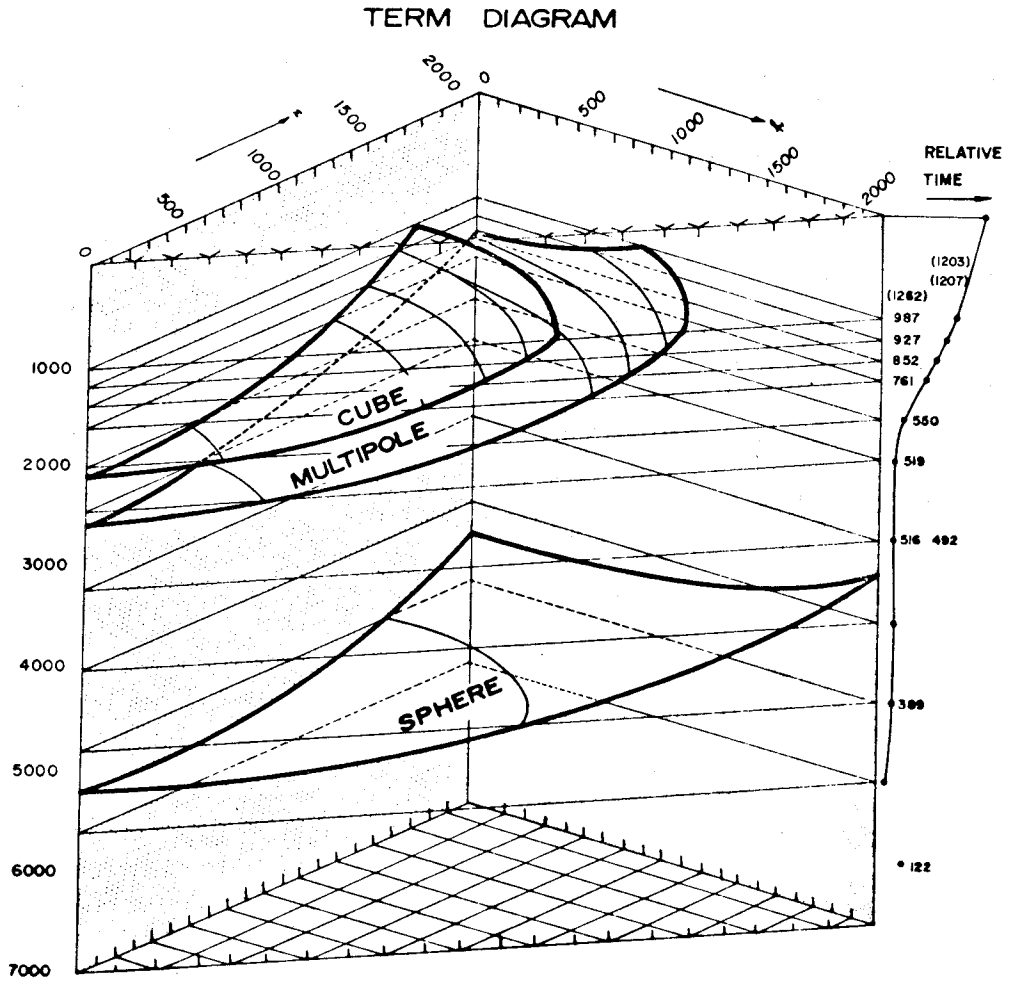

Figure 7.

5. Conclusions

While the expansion of the gravitational field in terms of multipoles has been used successfully for a number of years, it has up to now been neglected in the forward problem. It has here been shown to be an efficient method of calculating the gravity anomaly due to complex three-dimensional structures.

6. Acknowledgments

The authors wish to acknowledge the provision of a Macquarie University Research Grant to cover the computing costs involved.

7. References

BOTT, M.H.P. 1959 . The use of electronic digital computers for the evaluation of gravimetric terrain corrections. *Geophys.Prosp.* 7. 46-54

GOODACRE, A.K. 1973. Some comments on the calculation of the gravitational and magnetic attraction of a homogenous rectangular prism. *Geophys.Prosp.* 21. 66-69

GRANT, F.S. 1952. Three-dimensional calculation of gravitational anomalies. *Geophysics.* 17. 344-364

MACROBERT, T.M. 1967. *Spherical Harmonics.* Pergamon,New York.

NAGY, D. 1966. The gravitational attraction of a right rectangular prism. *Geophysics.* 31, 362-371

ST JOHN, V.P. & GREEN, R. 1967. Topographic and isostatic corrections to gravity surveys in mountainous areas. *Geophys.Prosp.* 15, 151-162

TAKIN, M. & TALWANI, M. 1966. Rapid computation of the gravitational attraction of topography on a spherical earth. *Geophys.Prosp.* 14. 119-142

TALWANI, M. & EWING, M. 1960. Rapid computation of gravitational attraction of three-dimensional bodies of arbitrary shape. *Geophysics.* 25. 203-225

8. Appendix

The expansion for the potential, due to an arbitrary volume v of density ρ

$$U = G\rho \int_v \frac{\rho dv}{|\vec{R}-\vec{r}|}$$

can be derived as follows.

Expanding the reciprocal distance, $|\vec{R}-\vec{r}|$, in terms of the Legendre functions (MACROBERT, 1967, p79) yields

$$U = \frac{G\rho}{R} \int_v \sum_{n=0}^{\infty} \left(\frac{r}{R}\right)^n P_n(\cos\gamma)\, dx'dy'dz'$$

where $R = (x^2 + y^2 + z^2)^{\frac{1}{2}}$, $r = (x'^2 + y'^2 + z'^2)^{\frac{1}{2}}$ and $\cos\gamma$ is as previously (Figure A1).

Let (R, θ, ϕ) be the spherical polar coordinates of the observation point (x, y, z) and (r, θ', ϕ') those of the point of integration (x', y', z').

Since (MACROBERT 1967,p.128)

$$P_n(\cos\gamma) = P_n(\cos\theta)\, P_n(\cos\theta') + 2 \sum_{m=1}^{n} \frac{(n-m)!}{(n+m)!} \cos m(\phi-\phi') \times$$

$$P_n^m(\cos\theta)\, P_n^m(\cos\theta').\cos m(\phi-\phi'),$$

$$U = \frac{G\rho}{R} \int_V \sum_{n=0}^{\infty} \left(\frac{r}{R}\right)^n P_n(\cos\theta)\, P_n(\cos\theta') + 2 \sum_{m=1}^{n} P_n^m(\cos\theta)$$

$$P_n^m(\cos\theta')\ \cos m(\phi-\phi')\ dx'\, dy'\, dz'$$

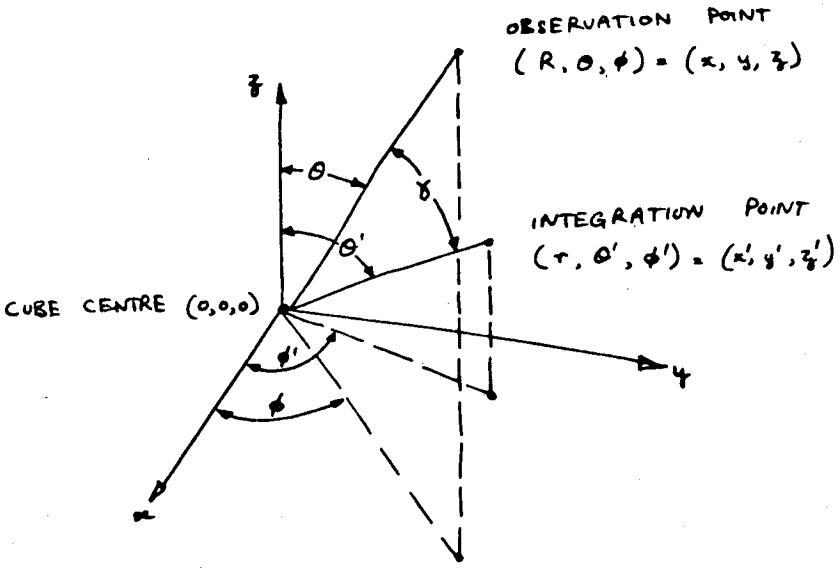

Figure A1. Coordinate Transformation

The origins of the coordinate systems are at the centre of the cube whose sides are parallel to the rectangular coordinates and of length a. By noting that

$$P_n^m(x) = (1 - x^2)^{m/2} \frac{d^m}{dx^m} P_n(x) \qquad \text{and}$$

$$P_n(x) = \frac{1}{2^n n!} \frac{d^n}{dx^n} (x^2 - 1)^n ,$$

the integration can be performed by interchanging the order of summation and integration and transforming back to the rectangular coordinate system (Figure A1)

$$\therefore \quad U = G\rho \left[\frac{a^3}{R} + \frac{7}{60} \frac{a^7}{R^9} \frac{1}{2^4} \left[3R^4 - 5\,(x^4 + y^4 + z^4) \right] \right]$$

9. Discussion

QURESHI: Do you specify an error for one calculation or for the whole series of calculations, as you will calculate the effect of a number of block elements for your model at a point? That means in any of your calculations you will have a total error. How would you describe this ?

STACEY: If I understand your question correctly, I think you are only concerned with fractional errors which cant be large.

QURESHI: You can specify that the error of your calculation at a point be less than 0.1 mgal. You are going to calculate at this point the effect of 100 elements which constitute your model. You can have a hundred errors. How would you specify the individual errors?

JOHNSON: If you have relative errors, you can work out the effect of each error. An error of a tenth mgal can be added, say, every ten times. You work out the maximum possible error in each calculation. The final error is the sum.

UNIDENTIFIED: Have you run an analysis program?

JOHNSON: No; we have been running against an exact calculation by the Nagy method.

KAULA: The same formulae can be found in *Theory of the Potential* by MacMillan.

JOHNSON: The one I used is at least a factor of ten more accurate than the computer software.

ANDERSON: I have been using similar formualae, and with regard to the references given by JOHNSON, all formulae are given in detail by MACMILLAN (*The Theory of the Potential*. Dover,New York)

JOHNSON: The development here is in the design of the type of convolution involved.

ANFILOFF, W.
SHAW, R.D.
Bureau of Mineral Resources
Department of Minerals & Energy
Canberra, ACT 2600
Australia

Proc.Symposium on Earth's Gravitational Field & Secular Variations in Position (1973),273-289.

THE GRAVITY EFFECTS OF THREE LARGE UPLIFTED GRANULITE BLOCKS IN SEPARATE AUSTRALIAN SHIELD AREAS

ABSTRACT

The three biggest linear gravity features on the Australian continent have a common form, and are an order of magnitude larger than any anomalies of comparable origin in Australia with the possible exception of the Perth Basin. They correspond with three belts of Proterozoic deformation involving narrow zones of crustal uplift, coupled with downwarping and the interpreted formation of large granulite batholiths on both sides. The development of all three belts appears to have been controlled by two major north-trending crustal dislocations.

Model studies of the gravity anomaly at the Fraser Range, south-western Australia, suggest that the Fraser Range mafic granulite has been thrust upward at least 4 km through granitic cover, with no corresponding displacement in the Conrad and Mohorovicic Discontinuities below the granulite. Two major granites on either side of the granulite are both interpreted as terminating at about 12 km.

Model studies of the anomalies in central Australia aid in delineating the southern Arunta and Musgrave upthrust granulite blocks and suggest the possible presence of four large bodies of granite and metasediment which terminate at a common depth horizon, possibly the Conrad Discontinuity. The horizon is interpreted as relatively flat. Because no gravity interpretation is unique, other models of the central Australian region which explain the gravity anomalies in terms of crustal warping or thrusting are also plausible. The models presented here are acceptable alternatives because they are consistent with the observation by Cleary of a Conrad Discontinuity at an average depth of about 20 km in many parts of Australia, and a crustal thickness which does not vary more than 5 km from an average value of about 40 km.

The termination of the gravity features associated with the southern Arunta granulite abruptly eastwards against a pronounced gravity lineament is taken to imply that a north-south compression was the cause of deformation, and that stress was released across a major crustal dislocation.

There is geological evidence of compressive events in the central Australian region at approximately 1700, 1000, 600 and 300 m.y., all consistent with stresses resulting from a primary north-south compression vector acting through central Australia. The permanence of a principal compression direction would be a limiting factor for theories of continental drift involving the rotation of the Precambrian Australian plate relative to its surroundings.

1. Introduction

This paper deals with the gravity anomalies associated with the Fraser Range, Musgrave, and southern Arunta mafic granulitic belts located in southwest and central Australia (figure 1). In terms of amplitude and length, these are three of the biggest linear gravity features in Australia, and are prominent on the gravity map of Australia (figure 2).

The systematic reconnaissance gravity coverage of most of Australia has enabled the anomalies to be compared with other gravity features, and their common characteristics to be assessed. Three belts of gravity anomalies are recognized. Each consists of a gravity ridge flanked by gravity troughs and each corresponds to a deformed belt consisting of an upthrust mafic granulite block flanked by combinations of granite and sediment. These are referred to as the Fraser Range, Musgrave, and southern Arunta Gravity Belts and Deformed Belts respectively. A model is suggested for the three structural belts

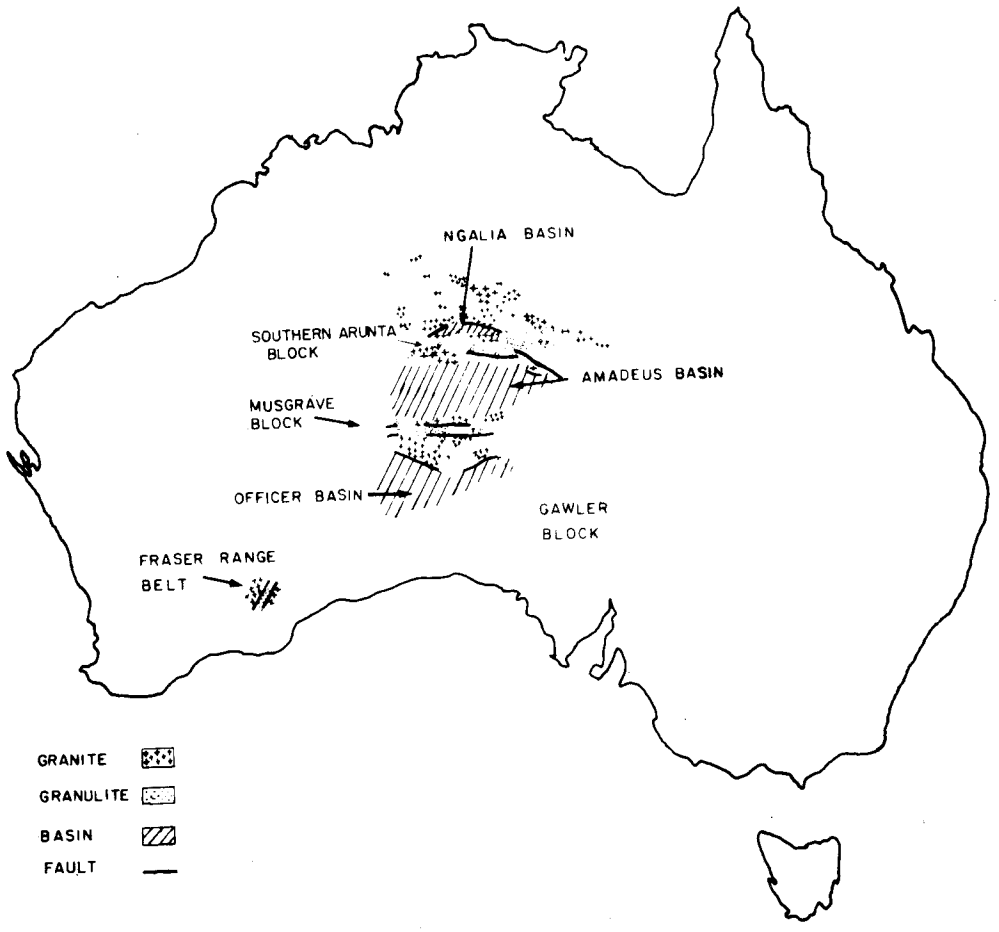

Figure 1. Granites, Granulites and Sedimentary Basins in Central and Southwestern Australia

which explains their present structure, and has some far-reaching, though speculative, implications.

Gravity profiles across the Fraser Range Gravity Belt along sections F1-F5 are shown in figure 3, and profiles across the Musgrave and southern Arunta Gravity Belts along sections C0-C5 in figure 4. The profiles of all three belts have a similar form, maintained over large distances. The maximum peak-to-trough amplitude is 170 mgal and gradients reach 4 mgal/km. In relation to the gravity levels in surrounding areas, the anomalies reach 60 mgal above and 110 mgal below surrounding levels.

Whereas the gravity ridges can be directly attributed to narrow zones of crustal uplift resulting in the exposure at the surface, of belts containing a major component of mafic granulite at the surface (MARSHALL & NARAIN 1954), the adjacent gravity lows have been interpreted in various ways. EVERINGHAM (1966) attributes the low east of Fraser Range to a granite 10 km thick; FLAVELLE (1965) explains the major low associated with the Ngalia Basin, N.T., mainly in terms of granite; MILTON & PARKER (1973) attribute the major low in the eastern part of the Officer Basin, S.A., mainly to a sediment in a basement trough with a 0.45 g cm^{-3} density contrast; and MATHUR (in prep.) attributes all four major lows in the central Australia region mainly to downwarping of the lower crust, based on the original concept

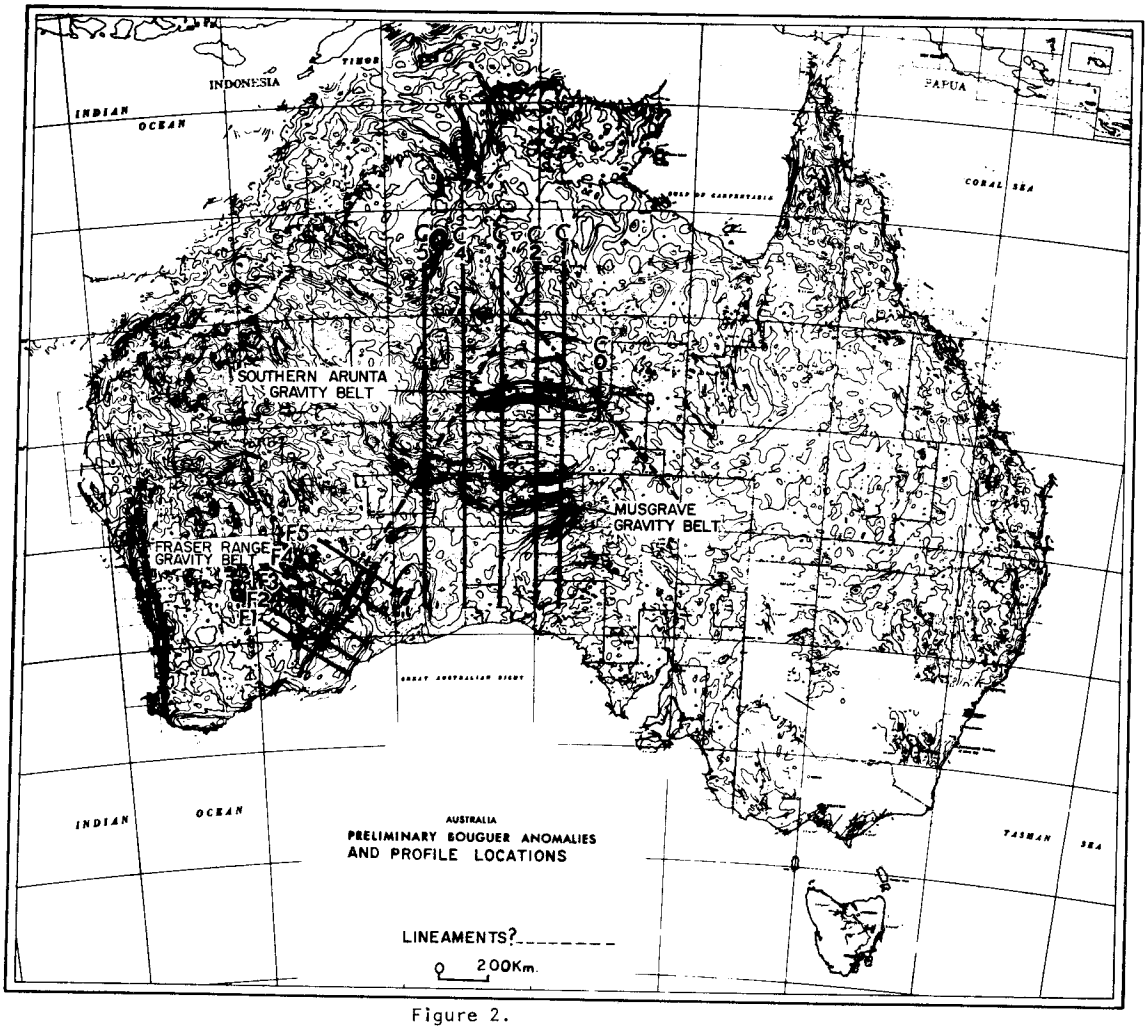

Figure 2.

of MARSHALL & NARAIN (1954) and Forman (in WELLS ET AL 1970; FORMAN & SHAW 1973). The crustal models shown in figures 5 and 9 explain the Bouguer anomalies in terms of density contrasts between rock units within the upper 20 km of the crust. However, because interpretations of gravity data are seldom unequivocal, a model such as that of MATHUR (in prep.) involving crustal warping is equally plausible in terms of available data. In the gravity models shown in figures 5 and 9, the local interpretations of granite made by EVERINGHAM (1966) and FLAVELLE (1965) have been extended with some modifications to all six major lows. The lows are postulated to have been caused by large blocks of low-density material consisting of granitic rock and variable amounts of metasediments overlain in the central Australian region by sedimentary basins. The distribution of exposed granitic rocks is sketched in figure 2. Granites and low density metasediments account for the bulk of exposed rock in the area corresponding to the greater part of the gravity low north of the Ngalia Basin. Similar rocks occur along the northern margin of the Amadeus Bsin and include large batholiths in the Mount Liebig and Mount Rennie 1:250,000 Geological Sheet areas. Large granitic bodies also crop out at the southern margin of the Amadeus Basin near Kulgera and at the northern margin of the Officer Basin in the Birksgate and Lindsay 1:250,000 Geological Sheet areas.

Two interpreted sections are presented, one across the Fraser Range Deformed Belt, and one across

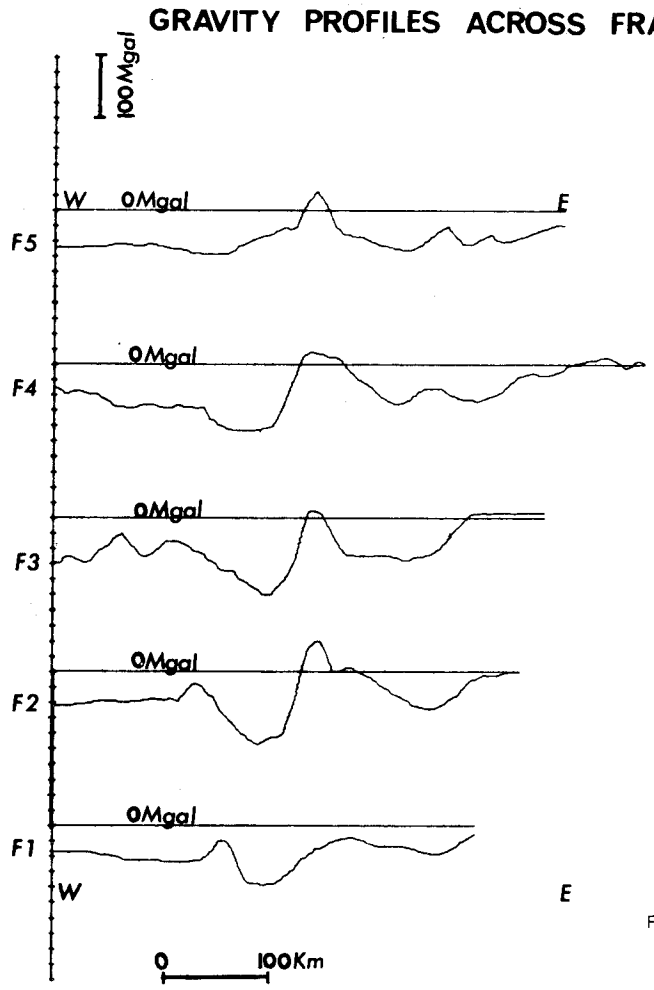

Figure 3

central Australia (the Central Australian Deformed Province) including the Musgrave and south Arunta Deformed Belts. Undeformed areas beyond the deformed belts are included in each section, so that the deformed belt structures can be interpreted in terms of mass variations relative to undeformed crustal layering.

The gravity ridges are interpreted in terms of varying amounts of mass excess caused by the uplift of granulites, and the lows are assumed to be substantially caused by large granitic bodies and variable amounts of metasediments extending down to specific depths. Large-scale compressive forces are postulated to cause the uplift of the granulite belts, subsidence and the preservation of low-density metasediments and older granites, and the formation of new granites.

2. Interpretation of the Fraser Range Gravity Belt in Southwestern Australia

The interpretation of the anomalies associated with the Fraser Range Deformed Belt is made along section F2, taken across the belt (figure 2). This particular section was chosen because detailed gravity information is available along it and the geology is better known than elsewhere in the Fraser Range. The section length is 300 km and includes Archaean gneisses and greenstones of the Yilgarn

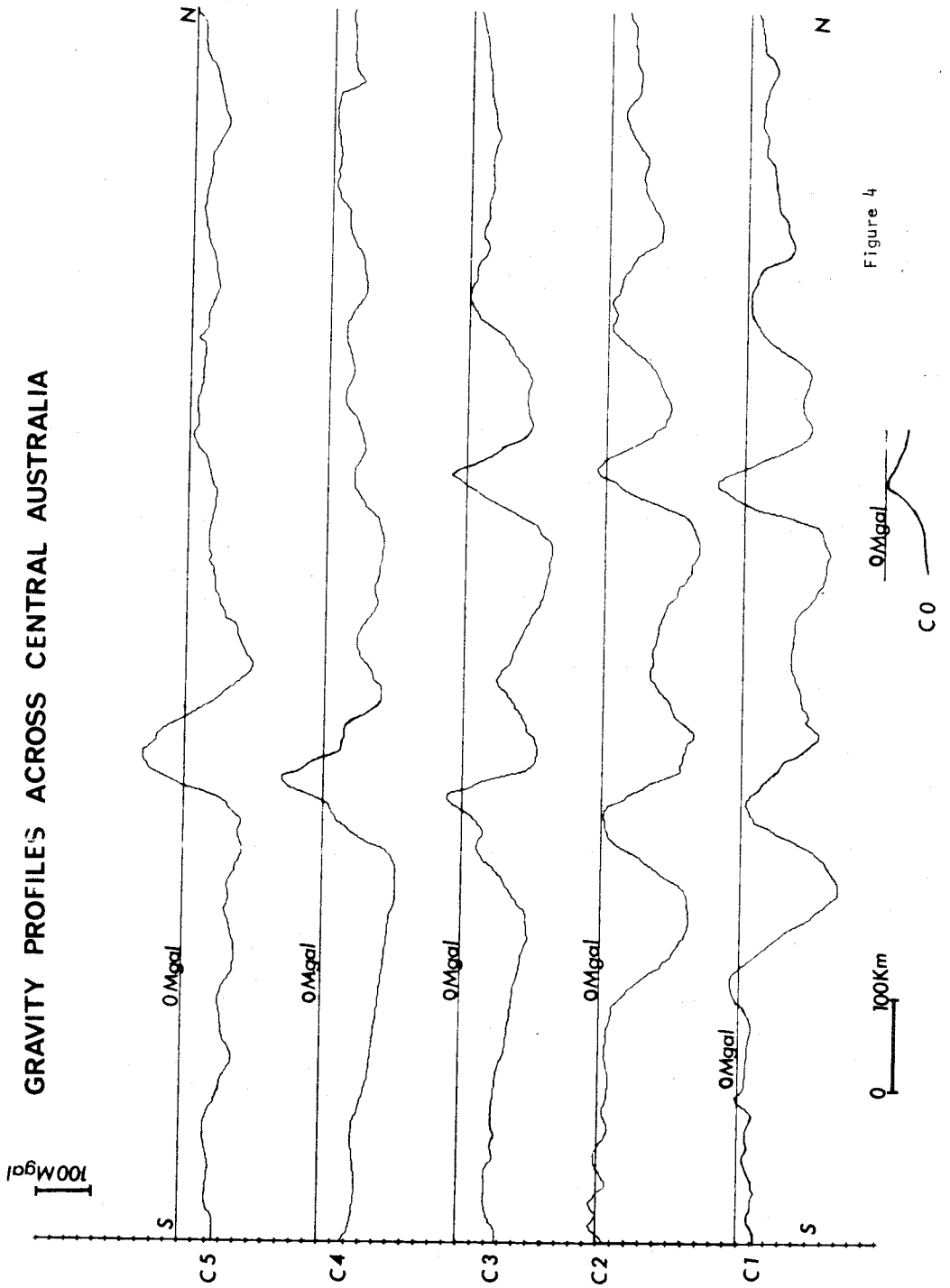
GRAVITY PROFILES ACROSS CENTRAL AUSTRALIA
100Mgal
N
S
0Mgal
C5
C4
C3
C2
C1
C0
0
100Km

Figure 4

FRASER RANGE GEOLOGY
AND INTERPRETED SECTION
- LINE F2

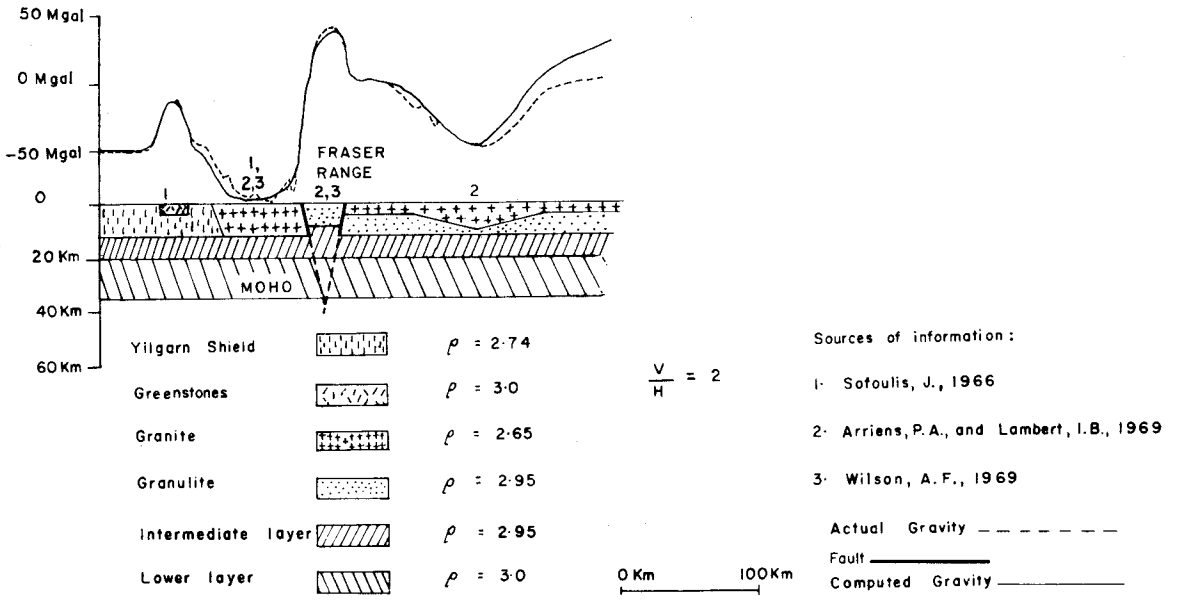

Figure 5

Shield in the west, Proterozoic granite, the Proterozoic Fraser Range mafic granulite, and the Balladonia granite and associated low-density rocks in the east.

The two granites and the mafic granulite may be interpreted as constituting a structural belt deformed against the Archaean shield by compression in the Proterozoic. Compression may have caused crustal buckling, resulting in the formation of two zones of subsidence flanking a zone of uplift. The subsidence is envisaged as causing the formation and preservation of large granite batholiths, and the uplift as causing the thrusting of mafic granulites into the upper levels of the crust. The upper part of the interpreted section (figure 5) is based on the geology of SOFOULIS (1966), WILSON (1969), and ARRIENS & LAMBERT (1969), and is modelled to consist of three main rock types:

- Archaean gneiss with a mean density of 2.74 g cm^{-3} to 12 km depth;
- two granitic bodies of density 2.65 g cm^{-3} both bottoming at about 12 km depth; and
- a mafic granulite of density 2.95 g cm^{-3}.

The lower part of the interpreted section depicts horizons at 20 and 35 km, based on the seismic results in the eastern part of the Yilgarn Shield (MATHUR in prep.), and also a subsurface granulite layer east of the Fraser Range.

The main features of the interpretation are:

1. The particular shape of the gravity anomaly over the Fraser Range granulite suggests that the granulite may have been thrust at least 4 km upwards through granitic cover.
2. The granites on either side of the Fraser Range granulite are present to a similar depth.
3. The very close agreement between the interpreted width of the Fraser Range granulite (33 km) and the mapped width (about 35 km) implies that the Conrad and Mohorovicic Discontinuities are both flat under the Fraser Range, as any upward displacement of these horizons would

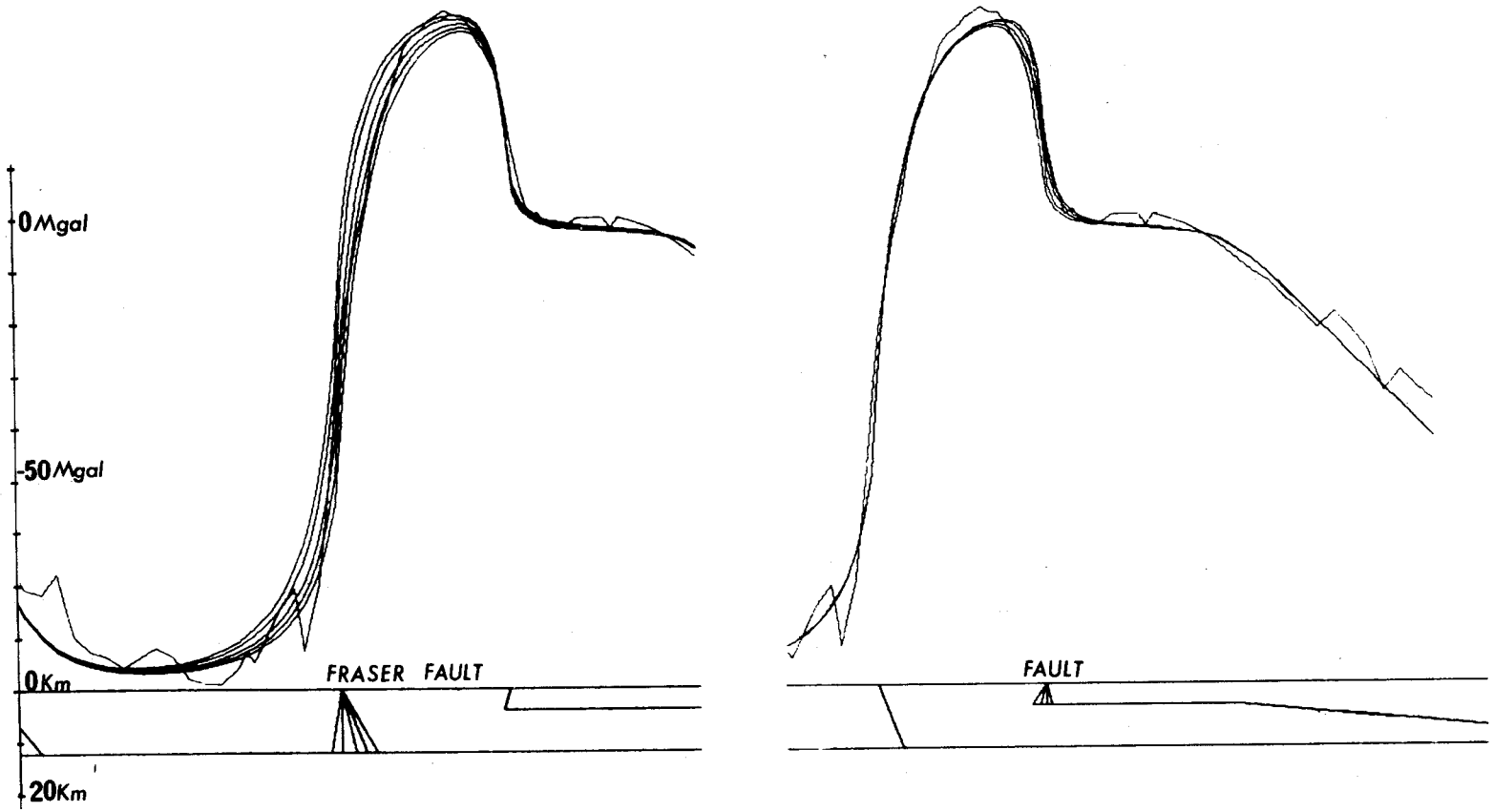

Figure 6. Sensitivity of the Computed Anomaly Over Fraser Range to Changes in the Fault Angles - Line F2

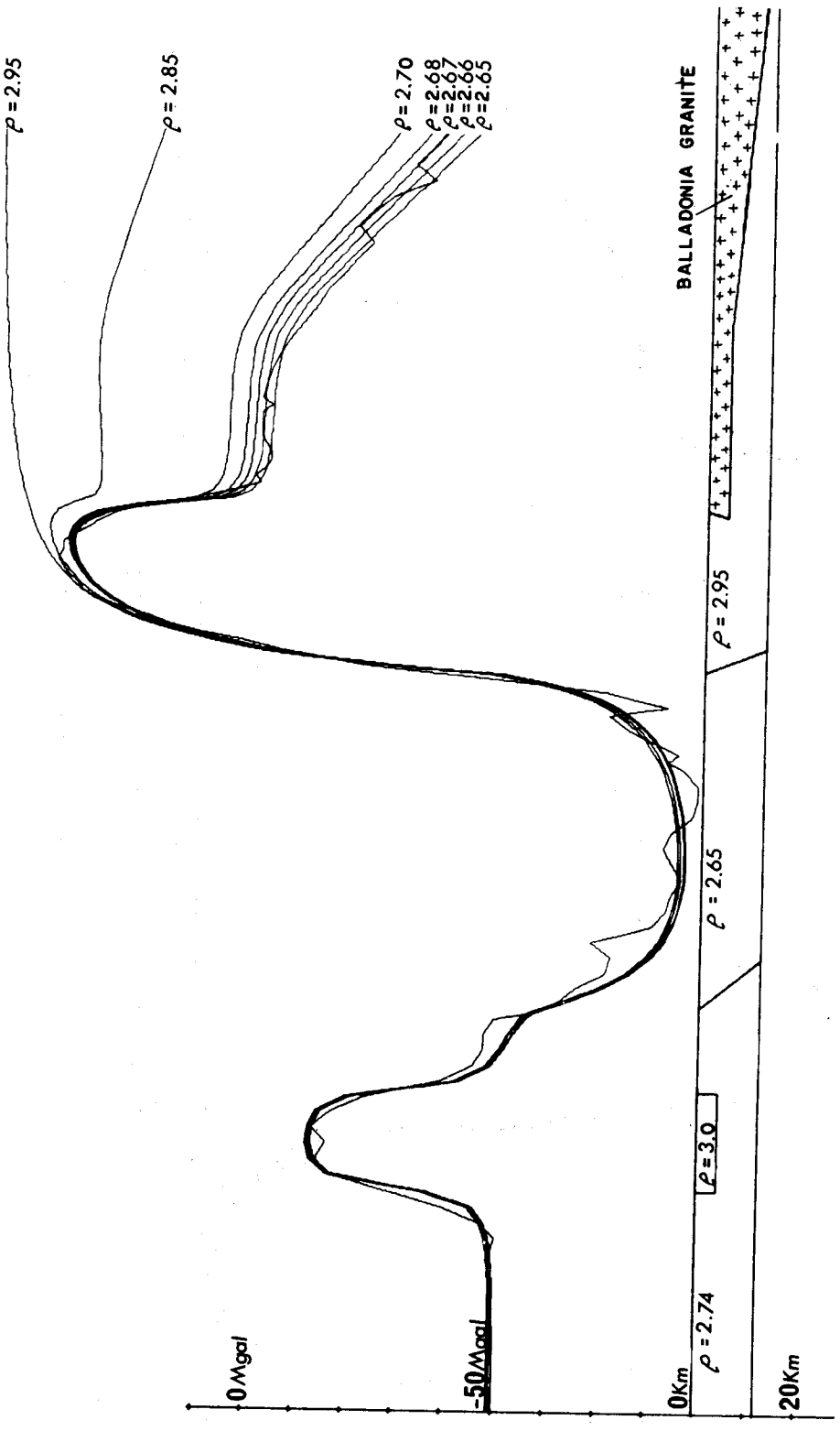

Figure 7. Sensitivity of the Computed Anomaly Over Fraser Range to Changes in the Density of the Balladonia Granite - Line F2

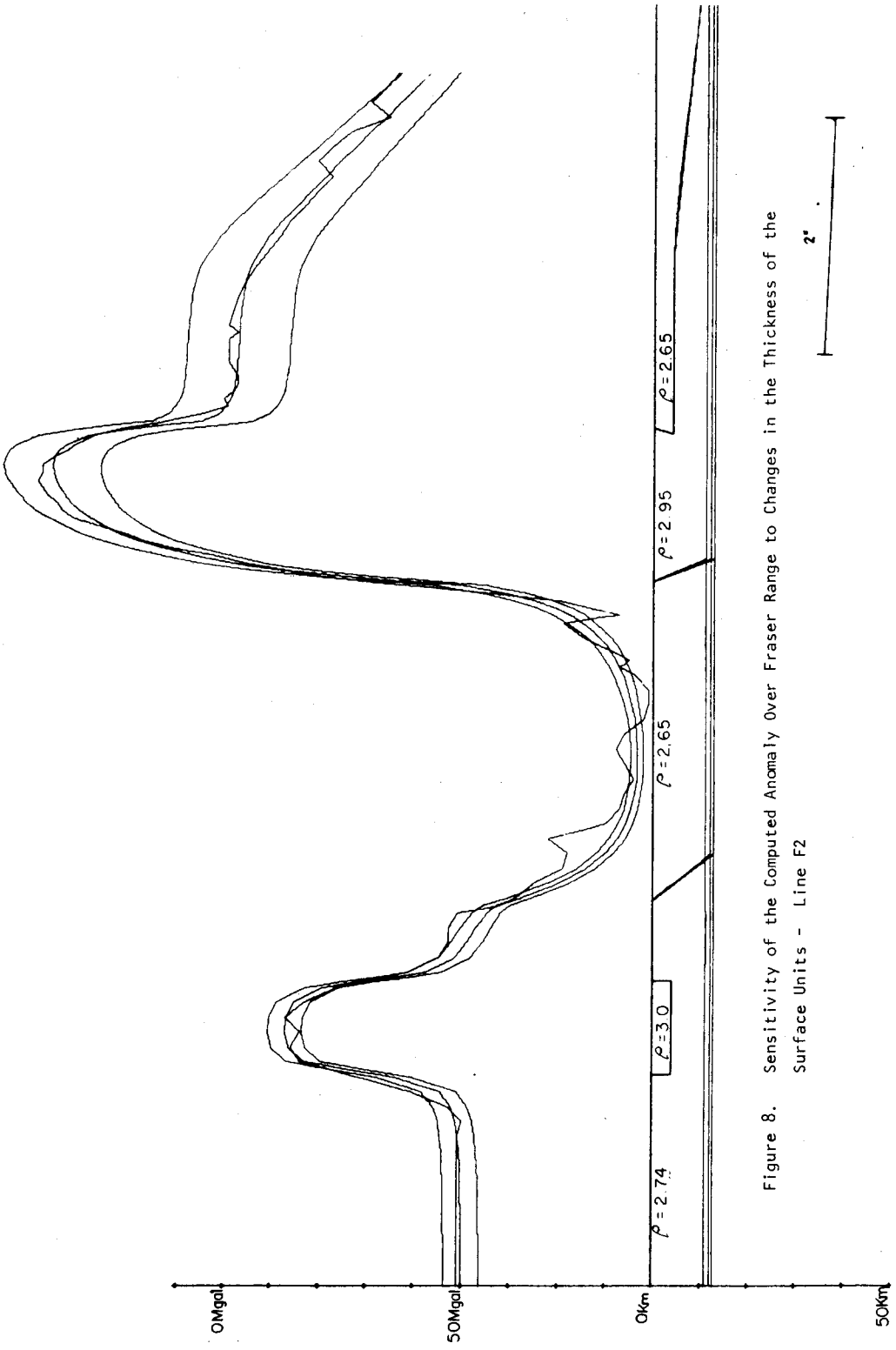

Figure 8. Sensitivity of the Computed Anomaly Over Fraser Range to Changes in the Thickness of the Surface Units - Line F2

constitute a mass excess at depth, and would have produced a much broader gravity anomaly over the granulite than is observed.

Figures 6, 7 & 8 are included to demonstrate the sensitivity of the computed anomaly to changes in various aspects of the interpreted model, and show the degree of resolution of the gravity modelling.

3. Interpretation of the Musgrave and Southern Arunta Gravity Belts in Central Australia

The Musgrave and Arunta Gravity Belts are interpreted along C1 (figure 1). This line is along 133° longitude and crosses the Gawler Block, the East Officer Basin, the Musgrave Block, the Amadeus Basin, the southern Arunta Block, the Ngalia Basin, and the northern Arunta Block. On the basis of the gravity effects, the area crossed is subdivided into two zones of undeformed crust, in the south and north, and two structural belts of deformation, the Musgrave and Arunta Deformed Belts (figure 9). The Officer Basin and its associated granites, the Musgrave Block upthrust granulites, and the southern Amadeus Basin and its associated granites are included in the Musgrave Deformed Belt. The northern Amadeus Basin and its associated granites, the upthrust granulites of the Arunta Block, and the Ngalia Basin and its associated granites are included in the southern Arunta Deformed Belt. Both belts may be considered to consist of two zones of subsidence flanking a zone of uplift, the subsidence being inferred from the accumulation of sediments, and the uplift from the presence of narrow zones of basic granulites in association with thrust faults.

Our interpretation of the gravity anomalies in central Australia assumesthat most of the gravity effects can be accounted for by density variation in the top 20 km of the crust (figure 9). The anomalies are interpreted in terms of lateral variation in density relative to two areas of undeformed crust at each end of the section. Assuming a mean crustal density of 2.81 g cm^{-3} to 20 km for the undeformed crust, the zones of subsidence can be considered to contain 20 km of granitic material of density 2.65 g cm^{-3}, and the zones of upthrust to contain crust of density 2.85 upthrust 5 km above its level in undeformed crust; and in the southern Arunta Block, 12 km of dense lower crustal material of density 3.0 g cm^{-3} all cratonized above the Conrad Discontinuity. The postulated Conrad Discontinuity at about 20 km in central Australia is consistent with its widespread distribution throughout many parts of the Australian continent (CLEARY 1973).

Three factors emerge from the interpreted model:

1. The similarity of gravity levels over undeformed crust at each end of the section is consistent with the crust there having a similar composition, and with the postulate that deformation in central Australia is intracratonic.
2. The gravity levels of all four gravity lows are consistent with equal thicknesses of low-density rock, interpreted as granite and lesser amounts of low-density metasediment in each case, over a distance of 600 km. This suggests that an essentially flat discontinuity, possibly the Conrad at 20 km depth, exists in the central Australian region.
3. The gravity levels over the upthrust zones suggest that up to 12 km of crustal uplift occurred along narrow zones relative to the undeformed crust, and that, if this caused displacements deeper in the crust, they have since been annulled by a process of density equilibration.

It is postulated that at about 1600-1700 m.y. (SHAW & STEWART 1973; MARJORIBANKS & BLACK 1973) in the

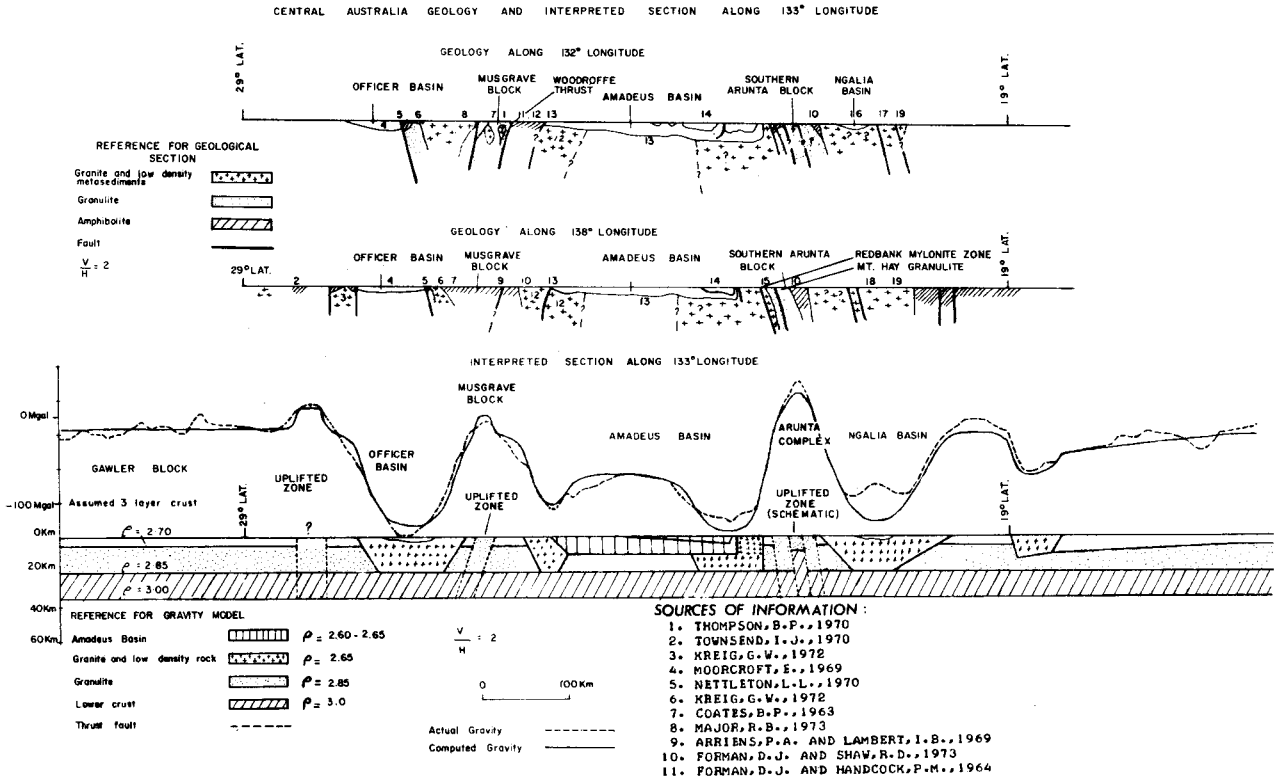

Figure 9

SOURCES OF INFORMATION :

1. THOMPSON, B.P., 1970
2. TOWNSEND, I.J., 1970
3. KREIG, G.W., 1972
4. MOORCROFT, E., 1969
5. NETTLETON, L.L., 1970
6. KREIG, G.W., 1972
7. COATES, B.P., 1963
8. MAJOR, R.B., 1973
9. ARRIENS, P.A. AND LAMBERT, I.B., 1969
10. FORMAN, D.J. AND SHAW, R.D., 1973
11. FORMAN, D.J. AND HANDCOCK, P.M., 1964
12. STEWART, A.J., 1967
13. YOUNG, G.A. AND SHELLEY, E.P., 1966
14. WELLS, A.T., FORMAN, D.J., RANFORD, L.C. AND COOK, P.J., 1970
15. MARJORIBANKS, R.W. AND BLACK, L.P., IN PREP.
16. WELLS, A.T., MOSS, F.J. AND SABITAY, A., 1972
17. WELLS, A.T., 1972
18. EVANS, T.G. AND GLIKSON, A.Y., 1969
19. SHAW, R.D. AND STEWART, A.J., IN PREP.

southern Arunta Deformed Belt and at 1000 m.y. or earlier (THOMSON 1970) in the Musgrave Deformed Belt, a strong north-south compressive stress caused the crust to buckle and consequently subside in two zones flanking a zone of uplift in a manner similar to that suggested by FORMAN & SHAW (1973). Anatectic granites are envisaged to have formed as sediments and perhaps older granites became deeply buried in the sinking troughs. Magmatic granites may also have formed at greater depths in the deformed zones. By the time crustal movements ceased, vast quantities of low-density material had accumulated to considerable depths. Conversely, in the zone of uplift, dense lower crustal material became cratonized in the upper levels of the crust. The southern Arunta Deformed Belt was reactivated, about 300-400 m.y. (IBID; SHAW & STEWART 1973) resulting in similar uplift and subsidence along roughly the same zones and the Musgrave Deformed Belt was similarly reactivated at about 600 m.y. (FORMAN *in* WELLS ET AL 1970; FORMAN & SHAW 1973).

It is postulated that after each main deformation the thickness of the structural units was reduced both by surface peneplanation and by their obliteration at depth due to large scale diffusion and largely vertical separation of elements particularly at about the level of migmatization. Additional equilibration of densities at depth might also be expected due to post-uplift phase changes in minerals as a result of adjustment to new PT conditions. Partial disruption of lateral density differences might be a result of granite intrusion late in the tectonic cycle. There is geological evidence that an event involving granite intrusion in the Musgrave Block between 1100-1200 m.y. (THOMSON 1970) extended to the southern Arunta Block as a migmatite event (MARJORIBANKS & BLACK 1973). No igneous activity is known to be associated with the later deformations considered to involve crustal warping and thrusting at 600 m.y. and 400-300 m.y. (FORMAN & SHAW 1973). Possibly the effective crustal strength was greater because the level of partial melting had, by that time, dropped to greater depths or because compression was maintained throughout the tectonic cycle. The continuous obliteration below a certain depth of the original density irregularities caused by the deformations may have produced a horizon that is conceivably the Conrad Discontinuity.

The gravity model shown in figure 9 is a much simplified representation of a complex history, but demonstrates how the gravity effects could be accounted for by density variations in the top 20 km of crust and how low-density rocks may terminate downwards at a common level.

4. Evidence for the Existence of a Primary North-South Compressive Force in Central Australia Over a 1400 m.y. Time Span

The causes of the uplift of the southern Arunta and Musgrave granulites are not known unequivocally, but circumstantial evidence suggests that the granulites of the southern Arunta Block were elevated by thrusting resulting from a strong north-south compressive force. Crustal buckling and fracturing in response to horizontal compressive forces has been proposed by MARSHALL & NARAIN (1954) to account for the main Bouguer anomaly features in the Central Australian Deformed Province. The marked similarilty in form, symmetry, and spatial periodicity of the main Bouguer anomaly features could be explained by such compressive deformation, especially if the initial buckles were formed during part of a continuous compressive episode. FORMAN & SHAW (1973) imply horizontal compression as a cause, but place more emphasis on overthrusting. Continuous or recurring compression would also help to explain the preservation of the original upthrust and downwarped crust, especially during any period of relative plasticity before the crust cooled and cratonized.

The eastern edge of the south Arunta Gravity Belt is truncated by a transverse lineament against which

both the gravity ridge and adjacent troughs are terminated abruptly. The change in gravity level of the ridge across the lineament is 50 mgal (figure 10). This aspect of the gravity anomalies suggests that the ridge and the two troughs were formed together as the result of an overall process of deformation, and that the overall deformation was terminated laterally by a crustal dislocation. This implies that the deformation is likely to have been caused by compressive stress acting on a relatively rigid plate, since only stress release across a dislocation would have sharply limited deformation along a lineament.

A similar dislocation would be expected to have occurred at the same time on the western side of the deformations, and there is evidence of a gravity lineament which extends from the Fraser Range Deformed Belt, past the western edge of the Musgrave and south Arunta Deformed Belts, and intersects the eastern lineament at a point centrally north of the Central Australian Deformed Province (figure 2). It is suggested that an exceptionally large primary north-south compressive force may have acted through the intersections of the two lineaments, causing the uplift of granulites and the subsidence of the flanking troughs.

Geological evidence indicates that the pattern of dominantly east-west structures in central Australia has been produced by a series of events involving overthrusting and overfolding which extended from the mid-Proterozoic to the mid-Carboniferous. In each event the geological structures can be interpreted to be the result of a major north-south compressive stress of constant orientation. There is evidence for the following events:

1700-1600 m.y. A major deformed zone (Redbank mylonite zone) separates the south Arunta granulites (Mt. Hay granulites) from an adjacent zone to the south containing migmatized granitic gneisses and low density metasediments. The mylonite foliation of the deformed zone is overprinted by a migmatite event at 1070 m.y. (concordant Rb/Sr total rock and mineral age - MARJORIBANKS & BLACK 1973). The gneisses have been dated at 1620 ± 70 m.y. (Rb/Sr total rock - OP.CIT.) and the uplift is possibl of this age or younger. Overthrusting consistent with compressive stress is suggested by the steep northerly dip of the mylonite foliation.

1000 m.y. or earlier Woodroofe Thrust is thought to be related to the intrusion of mafic and ultramafic igneous rocks (MAJOR 1973; THOMSON 1970) and related to structures in the granulites (COLLERSON, OLIVER & RUTLAND 1972), which have been dated at 1380 ± 120 m. y. by ARRIENS & LAMBERT (1969) (Rb-Sr total rock). Northerly directed overthrust and flattening suggests a primary north-south compressive stress.

600 m.y. The Petermann Range Nappe developed as a large recumbent anticline and complementary syncline involving both crystalline basement and sedimentary cover. Formation of the nappe at 600 m.y. is based on its stratigraphic relationships (FORMAN 1972) and Rb/sr mineral ages for metamorphosed granite intruding gneiss in the core of the nappe (LEGGO *in* FORMAN 1972). The extreme overfolding in a northerly sense is consistent with a major component of north-south compressive stress. The Woodroffe Thrust may have been reactivated during the 600 m.y. event (FORMAN & SHAW 1973).

300-400 m.y. Alice Springs Orogeny has been dated by K-Ar methods by STEWART (1971) and by Rb-Sr methods by ARMSTRONG & STEWART 1973). Deformation involved movement along a zone up to 10 km wide and the southward translation of a number of overthrusts in the northern margin of the Amadeus and Ngalia Basins (MARJORIBANKS & BLACK 1973; SHAW ET AL 1971). This implies a major component of north-south compressive stress.

In each event, the deformations produced are very elongate and regular. These large-scale yet narrow zones of uplift which developed with parallel orientation repeatedly over a time span of 1400 m.y. can be simply interpreted as the product of recurring compressive stress consistently oriented relative to the Central Australian Deformed Province.

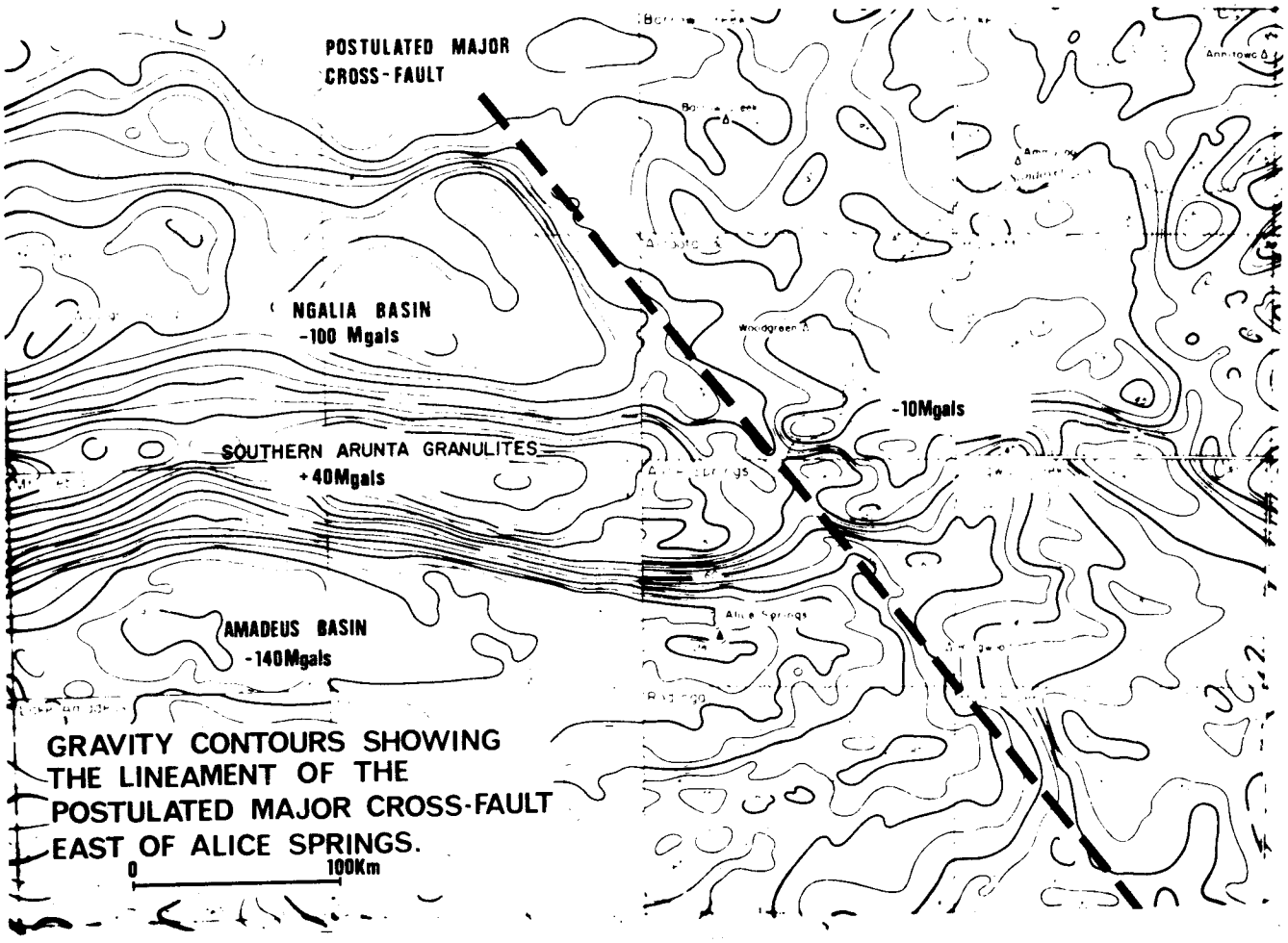

Figure 10

5. Conclusions

Three very similar structural belts, the Fraser Range, Musgrave, and southern Arunta Deformed Belts, and three corresponding belts of anomalies, the Fraser Range, Musgrave, and southern Arunta Gravity Belts are recognized. Each structural belt is interpreted as a narrow zone of uplift characterized by granulites and thrust faults and flanked by zones of subsidence characterized by sediments and large anatectic and magmatic granites. The three gravity belts have the same form and are an order of magnitude larger in amplitude than any other anomalies of comparable origin in Australia.

The Fraser Range interpretation indicates that two large granites flank the granulite. The large

gravity gradients across the faults bounding the granulite indicate that a sharp contact exists between it and the granites, suggesting that the granulite was thrust into a granitic cover. Both granites are interpreted as bottoming at about 12 km on each side of the granulite, and this may reflect the presence of a crustal horizon at that depth.

In particular, the Fraser Range anomaly negates the possibility of local uplift or warping at depth under the Fraser Range because the width of the anomaly closely matches the known width of the granulite. This strongly suggests that the Conrad and Mohorovicic Discontinuities are flat. The interpretation across central Australia suggests that the discontinuities are flat there also. Mass deficiencies caused by four postulated bodies consisting of granites and variable amounts of metasediment appear to terminate downwards at a common depth, and mass excesses caused by the uplift of the Musgrave granulites can also be placed above the common granite depth. This suggests that the granites and associated metasediments may terminate downwards at a flat discontinuity, possibly the Conrad Discontinuity at about 20 km depth, below which density irregularities do not occur.

Geological evidence suggests that the major east-west structures in central Australia were caused by a recurring primary north-south compressive stress over the interval 1700 - 300 m.y. We believe that compression can also be deduced from the gravity information. The prominent truncation of the gravity features at the eastern edge of the Central Australian Deformed Province suggests that a major NNW crustal dislocation terminated stress and resulting deformation farther eastwards. A similar dislocation is interpreted to extend north-north east from the Fraser Fault along the western edge of the Central Australian Deformed Province, and, if extrapolated, the two would intersect at a point centrally north of the deformed zone.

The deformation of the Fraser, Musgrave, and south Arunta belts can therefore be considered to have occurred between two intersecting major crustal dislocations. The interpreted relationship between the crustal dislocations and the Central Australian Deformed Province implies that the deformed province was an intracontinental feature from at least the time of formation of the 1700 m.y. old southern Arunta Deformed Belt.

There is evidence of deformations involving north-south compressive stress in the Central Australian Deformed Province at 1700, 1000, 600, and 300 m.y. Immediately after the main 1700 m.y. and 1000 m.y. deformations, anisotropy may have affected the direction of stress, but considering the length of time and the magnitude and consistency of the later strains involved, it is unlikely that anisotropy markedly affected the stress direction in the more recent events. The overall history of stress in the Central Australian Deformed Province therefore appears to be one of compressive stresses resulting from a more or less consistent north-south primary compression vector. This suggests that the main Australian Precambrian plate did not rotate relative to its surroundings if it underwent continental drift between 1700 and 300 m.y., since this would probably have produced new principal stress directions.

6. Acknowledgments

The authors wish to thank A.Y. Glikson, A.J. Stewart and R.W. Marjoribanks for their helpful comments on the initial manuscript.

This paper is published with the permission of the Director, Bureau of Mineral Resources, Geology & Geophysics, Canberra, ACT.

7. References

ARMSTRONG, R.L. & STEWART, A.J. 1973. Rubidium-Strontium Dates and Excess Argon in the Arltunga Nappe Complex, Northern Territory. *Bur.Min.Resour.Aust.Rec.* (in preparation),Canberra ACT.

ARRIENS, P.A. & LAMBERT, I.B. 1969. On the Age and Strontium Isotopic Geochemistry of Granulite-Facies Rocks from the Frazer Range, Western Australia, and the Musgrave Ranges, Central Australia. *Geol.Soc.Aust.Spec.Publ.* 2,377-388.

CLEARY, J. 1973. Australian Crustal Structure. *Tectonophysics* (in press).

COATES, R.P. 1963. The Geology of the Alberga 4-Mile Military Sheet. *Geol.Surv.S.Aust.Rep.Invest.* 22.

COLLERSON, K.D., OLIVER, P.L. & RUTLAND, R.W.R. 1972. An Example of Structural and Metamorphic Relationships in the Musgrave Orogenic Belt, in Central Australia. *J.geol.Soc.Aust.* 18, 379-393.

EVANS, T.G. & GLIKSON, A.Y. 1969. The Geology of the Napperby Sheet Area, Northern Territory. *Bur. Miner.Resour.Aust.Rec.* 1969/85, Canberra ACT.

EVERINGHAM, I.B. 1966. *Gravity Anomalies on the Precambrian Shield of Southwestern Australia.* M.Sc. Thesis, University of Western Australia, Perth WA.

FLAVELLE, A.J. 1965. Helicopter Gravity Survey by Contract, Northern Territory and Queensland. *Bur.Miner.Resour.Aust.Rec.* 1965/212,Canberra ACT.

FORMAN, D.J. 1972. Petermann Ranges, N.T. - 1:250,000 Geological Sheet. *Bur.Miner.Resour.Aust.explan. Notes* SG/52-1,Canberra ACT.

FORMAN, D.J. & HANCOCK, P.M. 1964. Regional Geology of the Southern Margin, Amadeus Basin, Rawlinson Range to Mulga Park Station. *Bur.Miner.Resour.Aust.Rec.* 1964/41,Canberra ACT.

FORMAN, D.J. & SHAW, R.D. 1973. Deformation of the Crust and Mantle in Central Australia. *Bur.Miner.Resour.Aust.Bull.* 144,Canberra ACT.

KRIEG, G.W. 1972a. Everard, S.A. - 1:250,000 Geological Map. *Geol.Surv.S.Aust.explan.Notes* SG/53-13, Adelaide SA.

KREIG, G.W. 1972b. The Ammaroodina Inlier. *Geol.Surv.S.Aust.Quart.geol.Notes* 41,Adelaide SA.

MAJOR, R.B. 1973. Woodroffe, S.A. - 1:250,000 Geological Map. *Geol.Surv.S.Aust.explan.Notes* SG/52-12,Adelaide SA.

MARJORIBANKS, R.W. & BLACK, L.P. 1973. The Geology and Geochronology of the Arunta Complex North of Ormiston Gorge,Central Australia. *Bur.Miner.Resour.Aust.Rec.* 1973/181, Canberra ACT.

MARSHALL, C.E. & NARAIN, N. 1954. Regional Gravity Investigations in the Eastern and Central Commonwealth. *Mem.* 1954/2,Department of Geology & Geophysics,University of Sydney,Sydney NSW.

MATHUR, S.P., BRANSON, J.C. & MOSS, F.J. 1973. Geotraverse Seismic Survey, W.A. *Bur.Miner.Resour. Aust.Rec.* (in preparation),Canberra ACT.

MATHUR, S.P. 1973. A Proposal for Deep Crustal Seismic Sounding Survey in Central Australia. *Bur. Miner.Resour.Aust.Rec.* (in preparation),Canberra ACT.

MILTON, B.E. & PARKER, A.J. 1973. An Interpretation of Geophysical Observations on the Northern Margin of the Eastern Officer Basin. *Geol.Surv.S.Aust.Quart.geol.Notes* 46,Adelaide SA.

MILTON, B.E. & THORNTON, R.C.N. 1970. Discovery of a Dense Lower to Middle Palaeozoic Dolomite in the Northwest Arckaringa Basin. *Geol.Surv.S.Aust.Quart.geol.Notes* 36,Adelaide SA.

MOSSFROFT, E. 1969. Sesmic Reflection, Refraction and Gravity Survey,Eastern Officer Basin, 1966. *Min.Rkv.Adelaide* 126,58-70.

NETTLETON, L.L. 1970. *Eastern Officer Basin Gravity Survey PEL 10 & 11, South Australia.* Geophysical Associates Pty Ltd, Report for Murumba Oil N.L. (S.Aust.Dept. Mines open file Env.1196),Adelaide SA.

SOFOULIS, J. 1966. Widgemooltha, W.A. - 1:250,000 Geological Map. *Geol.Surv.W.Aust.explan.Notes* SH/51-14,Perth WA.

SHAW, R.D. & STEWART, A.J. 1973. Regional Geology of the Precambrian Arunta Block. In *Economic Geology of Australia and Papua and New Guinea.* Australian Institute of Mining and Metallurgy,Melbourne Vic.

SHAW, R.D., STEWART, A.J., YAR KHAN, M. & FUNK, J. 1971. Progress Reports on Detailed Studies in the Arltunga Nappe Complex, N.T., 1971. *Bur.Miner.Resour.Aust.Rec.* 1971/66,Canberra ACT.

STEWART, A.J. 1967. Kulgera, N.T. - 1:250,000 Geological Series. *Bur.Miner.Resour.Aust.explan.Notes* SG/53-5,Canberra ACT.

STEWART, A.J. 1971. K-Ar dates from the Arltunga Nappe Complex,Northern Territory. *J.geol.Soc.Aust.* 17,205-211.

THOMSON, B.P. 1970. A Review of the Precambrian and Lower Palaeozoic Tectonics of South Australia. *Trans.R.Soc.S.Aust.* 94,193-221.

TOWNSEND, I.J. 1970. Stratigraphic Drilling Programme 1969. Western Archaringa Basin. *S.Aust.Dep. Mines Rep.* BK70/40,Adelaide SA.

WELLS, A.T., FORMAN, D.J, RANFORD, L.C. & COOK, P.J. 1970. Geology of the Amadeus Basin, Central Australia. *Bur.Miner.Resour.Aust.Bull.* 100,Canberra ACT.

WELLS, A.T., MOSS, F.J. & SABITAY, A. 1972. The Ngalia Basin, Northern Territory - Recent Geological and Geophysical Information Upgrades Petroleum Prospects. *APEA J* 12,144-151.

WELLS, A.T. 1972. Mount Doreen, N.T. - 1:250,000 Geological Series. *Bur.Miner.Resour.Aust.explan. Notes* SF/52-12,Canberra ACT.

WHITWORTH, R. 1970. Reconnaissance Gravity Survey of Parts of Northern Territory and Western Australia, 1967. *Bur.Miner.Resour.Aust.Rec.* 1970/15,Canberra ACT.

WILSON, A.F. 1969. Granulite Terrains and Their Tectonic Setting and Relationship to Associated Metamorphic Rocks in Australia. *Geol.Soc.Aust.Spec.Publ.* 2,243-258.

YOUNG, G.A. & SHELLEY, E.P. 1966. The Amadeus Basin Airborne Magnetic and Radiometric Survey, N.T. *Bur.Miner.Resour.Aust.Rec.* 1966/64,Canberra ACT.